PELLIZZARI, SARAH. M.S. Firing Rate Homeostasis Through the Co-Expression of Two Feedback Mechanisms that Detect Separate Aspects of Neuronal Activity. (2022) Directed by Dr. Joseph Santin. 56 pp.

How do neurons produce consistent patterns of electrical activity throughout life? Foundational studies suggest neurons self-regulate activity through molecular feedback loops that track a single cellular variable whose dynamics mirror firing rate, such as Ca^{2+}, Na^{+}, or voltage over both long and short timescales. The low affinity Na^{+}/K^{+}ATPase, termed the dynamic Na^{+}/K^{+}ATPase, which tracks intracellular Na^{+}, has emerged as an activity regulator over the span of approximately one minute by producing the ultraslow afterhyperpolarization (usAHP) in spinal locomotor circuits. In this study, we sought to investigate the role of the dynamic Na^{+}/K^{+}ATPase in regulating the activity of neurons that produce breathing using vagal and hypoglossal respiratory motoneurons. Here we report that vagal motoneurons have an usAHP, while hypoglossal motoneurons do not. Despite having a phenotype similar to the locomotor usAHP, the usAHP in respiratory vagal motoneurons is generated not only by the dynamic Na^{+}/K^{+}ATPase but also by voltage-dependent recruitment of Kv7 channels. Furthermore, both mechanisms are variably expressed across populations of neurons but have an inverse functional relationship from cell to cell (when the dynamic Na^{+}/K^{+} ATPase is high, Kv7 is low and vice versa). Both the dynamic Na^{+}/K^{+}ATPase and Kv7 channels regulate firing rate through activity-dependent feedback during physiological bursting, with the contribution of each reciprocally balanced. These findings reveal that neurons can use various combinations of different feedback signals to defend firing rate set-points and highlight the potential for difficulty in defining global homeostatic rules even within a population of neurons that give rise to the same behavior.

FIRING RATE HOMEOSTASIS THROUGH THE CO-EXPRESSION OF TWO FEEDBACK MECHANISMS THAT DETECT SEPARATE ASPECTS OF NEURONAL ACTIVITY

by

Sarah Pellizzari

A Thesis

Submitted to

the Faculty of The Graduate School at

The University of North Carolina at Greensboro

in Partial Fulfillment

of the Requirements for the Degree

Master of Science

Greensboro

2022

Approved by

Dr. Joseph Santin
Committee Chair

APPROVAL PAGE

This thesis written by Sarah Pellizzari has been approved by the following committee of the Faculty of The Graduate School at The University of North Carolina at Greensboro.

Committee Chair

Dr. Joseph Santin

Committee Members

Dr. Malcolm Schug

Dr. John Tomkiel Dean

July 8, 2022

Date of Acceptance by Committee

July 8, 2022

Date of Final Oral Examination

ACKNOWLEDGEMENTS

In no particular order I would like to acknowledge the following people: Min Hu, Dr. Joseph Santin, Dr. John Tomkiel Dean, Dr. Malcolm Schug, Dr. Lara do Amaral Silva, Dr. Sandy Saunders, Dr. Michael Gray, and Nikolaus Bueschke. Thank you to Drs. Tomkiel Dean and Schug for serving on my committee and for their help in making this whole thing happen. To the members of the Santin Lab, Drs. Amaral-Silva, Saunders, Gray, and Nikolaus, thank you for the endless technical support and frog care assistance. A special thank you to Drs. Amaral-Silva and Gray for making the physiological protocol a reality. Thank you to Min Hu, who put up with my frustrations in the editing process of this manuscript first-hand, as well as being an amazing partner who supported me in all ways while I completed the experiments for this project, which occasionally ran for 18 hours. I could not have done any of this without you and your encouragement and listening ear. Lastly, but certainly not least, I extend my gratitude to Dr. Joseph Santin who has been an incredible mentor and has set a remarkably high bar for my next PI. While it was most certainly frustrating to hear the words “your dialing wasn’t right” and “did you check the membrane potential”, this caused me to realize the value of setting high standards for the work I do. While critical, Dr. Santin was also the first and most excited to see the first cell to do something cool and always available to lend a helping hand (seriously, you could reach him in the car, in a plane, at all hours). I know this did not work out like any of us had planned, but I do not regret the time spent in this lab, at this University, with all of these incredible people. You all have made me a better person and scientist and I am insanely grateful.

TABLE OF CONTENTS

LIST OF FIGURES

CHAPTER I: INTRODUCTION

Neurons must produce stable outputs to ensure proper function and survival of the organism. When this does not occur, neurological disorders such as epilepsy arise (Lignani et al., 2020). The ability for neurons to produce stable outputs ultimately depends on their ability to fire electrical impulses (action potentials) at the correct time and frequency, which is determined by the neuron's intrinsic properties (the expression of ion transporters and the physical properties of the cell membrane). Therefore, intrinsic properties, in tandem with a neuron's synaptic inputs, define the function of any neuron (Marder & Goaillard, 2006). The study of the intrinsic properties of neurons allows us to understand the mechanisms by which they produce and maintain stable patterns of activity, which is critical to the health of all animals, and may go awry in many neurological disorders.

Regulation of Excitability

For neurons to produce stable outputs, the ease or difficulty of action potential generation (termed "excitability") must be tightly regulated. Excitability is an intrinsic property, therefore the study of the ease or difficulty of action potential generation is known as the study of intrinsic excitability.

Feedback homeostasis, which is based on the engineering principle of control theory, has provided the main framework for understanding the regulation of many physiological systems, including intrinsic excitability (LeMasson et al., 1993; Wiener, 2019). For neurons, the general framework for neuronal regulation involves the ability to sense firing rate and adjust ion channel function to maintain a set-point level of activity (LeMasson et al., 1993; O'Leary et al., 2014; G. Turrigiano et al., 1994). Biologically, activity is thought to be decoded by a sensory system that monitors biochemical or biophysical variables that mirror the neuron's fire rate, typically intracellular Ca^{2+} transients that closely track mean firing rate. When firing rate drifts away from the set-point, changes in intracellular Ca^{2+} trigger a cellular response that adjusts ion

channel function to recover the set-point. These adjustments that restore excitability generally occur in the form of transcription-based responses that synthesize and traffic ion channels to the cell membrane (Trasande & Ramirez, 2007), but also involve translation and post-translational modifications. Research that began with computational neuron models based on control theory suggests there must be only one activity sensor that detects a neuron's activity and causes the downstream processes necessary to adjust the neuron's activity (Marder & Prinz, 2002; O'Leary et al., 2014). The use of a single activity sensor prevents a phenomenon known as "windup" that can occur in dynamical systems (O'Leary et al., 2014). Windup occurs when there are multiple sensors that defend even slightly different set points, which prevents the system from satisfying all target points of each sensor at one time. This leads to simultaneous adjustments in an attempt to regulate each different set point, ultimately resulting in the loss of regulation from the intended target (O'Leary et al., 2014). In computer models, the addition of a second sensor/target has resulted in windup (O'Leary et al., 2014). While it is possible that neurons could use more than one activity sensor (Z. Liu et al., 1998), this has not yet been observed biologically.

The activity sensor in the majority of systems, in both short-term and long-term regulation of intrinsic excitability, has been shown to be intracellular Ca^{2+} (Cao et al., 2015; Ha et al., 2016; Ha & Cheong, 2017; Joseph & Turrigiano, 2017; Marder & Prinz, 2002). Intracellular Ca^{2+} is a well-suited sensor for activity, as Ca^{2+} enters the cell during membrane depolarization and is released from intracellular stores shortly after the action potential (Dwivedi & Bhalla, 2021). Therefore, intracellular calcium levels provide a biochemical readout of a neuron's current activity level. Additionally, Ca^{2+} is a versatile and powerful second messenger, capable of initiating kinase cascades and DNA transcription on its own to modulate a neuron's intrinsic properties and activity levels (Kaczmarek, 1987; Rasmussen & Barrett, 1984; Sheng & Greenberg, 1990). As neurons have activity set points, it follows that they may also have intracellular calcium concentration set points. In these cases, when firing rate changes, neurons

sense changes in their intracellular calcium and then alter the expression/function of ion channels to bring intracellular calcium back to the target value by altering the neuron's activity, thus maintaining excitability within an adaptive range (Joseph & Turrigiano, 2017; Nelson & Turrigiano, 2008). This process has been termed "homeostatic plasticity" and essentially allows neurons to recover their physiological activity when faced with large perturbations such as ion channel deletion, pharmacological blockade, or injury (Marder & Goaillard, 2006; O'Leary et al., 2014; G. Turrigiano et al., 1994).

Much of the work on homeostatic plasticity has been performed in the stomatogastric ganglion (STG) of crustaceans, the Drosophila neuromuscular junction (NMJ), and in various rodent circuits (Apostolopoulou & Lin, 2020; Borde et al., 1995; Marder & Goaillard, 2006). When removed from the animal or neuromodulatory input, the neurons of the STG lose their characteristic activity (Lett et al., 2017; G. Turrigiano et al., 1994; G. G. Turrigiano & Marder, 1993). However, they regain their activity if maintained for days in culture (Lett et al., 2017; G. Turrigiano et al., 1994). Turrigiano et al. (1994, 1995) found that the resumption of characteristic activity occurs because the neuron is able to correct for the lack of synaptic input by adjusting the relative ratios of certain ion channels in the membrane (G. Turrigiano et al., 1994, 1995). The important finding from this work is that neurons each appear to have a unique set point that they maintain autonomously. How exactly a neuron "knows" what its unique activity set point is has yet to be uncovered (Marder & Goaillard, 2006).

The study of homeostatic plasticity has also revealed how channels and their coding genes can interact with one another to maintain intrinsic excitability in the face of long term genetic, electrical, or pharmacological disturbances. For example, a K^+ current known as I_A which can be encoded by either the *shal* or *shaker* genes has been shown to persist in *shal*$^{-/-}$ mutants via a compensatory increase in *shaker* (Chen et al., 2006). Additionally, I_A and the Ca^{2+} activated K^+ current I_{KCa}, have been shown to be coupled both functionally and at the level of mRNA expression in neurons of the STG, but in a contradictory manner (Ransdell et al., 2012).

While decreases in I_A are accompanied by increases in I_{KCa} functionally, increases in I_A mRNA are associated with increases in I_{KCa} mRNA (Ransdell et al., 2012). I_{KCa} is not the only current with which I_A is correlated. Increases in I_A are compensated by an increase in the hyperpolarization activated mixed cation current, I_h (MacLean et al., 2005). Surprisingly, research has also shown that channels with related, but different functions can replace another channel that has been genetically removed. For example, in Drosophila *shal*$^{-/-}$ mutants, neurons of the NMJ have a large increase in I_{BKKCa} which is a current from the Ca^{2+}-activated big conductance K^+ channel (Bergquist et al., 2010).

Homeostatic plasticity has been shown to be effective at restoring a neuron's physiological activity in both computer models and real neurons. However, this process often takes between hours and days to be effective (Golowasch et al., 1999; G. Turrigiano et al., 1994, 1995; G. G. Turrigiano & Marder, 1993). Therefore, these mechanisms are likely too slow to constrain activity over time scales that are relevant for most neural circuits (Zenke & Gerstner, 2017). This is especially important for certain pathological states such as seizures, where aberrant overactivity must be corrected within seconds, not hours, for the organism to survive the event. Therefore, feedback mechanisms must act over shorter time scales, from seconds to minutes, to regulate the excitability of neurons and circuits. This is not to say that slower homeostatic mechanisms are not relevant or important. Rather, these slower forms of intrinsic excitability regulation coexist with the faster mechanisms to maintain neuronal activity within a tight range over long and short timescales.

Regulation of excitability over shorter timescales: The medium Afterhyperpolarization, Part I

One form of regulation that operates over short timescales is termed the "afterhyperpolarization". The afterhyperpolarization occurs after single or multiple action potentials and involves mechanisms that respond to recent activity by reducing the membrane potential below the resting level. Hyperpolarization of the membrane makes action potential

generation more difficult by moving the membrane further from the action potential threshold and interacting with other ion channels that make it harder to fire (Storm, 1989; Tiwari et al., 2019; H.-Y. Zhang & Sillar, 2012). Therefore, the afterhyperpolarization serves as a short-term negative feedback mechanism to reduce excitability following periods of high neuron activity (Tiwari et al., 2019). Afterhyperpolarizations (AHPs) can operate across different time scales and be engaged by different mechanisms, many of which are still incompletely understood and sources of confusion. The medium AHP, mAHP, occurs after one spike or after a cluster of action potentials called a burst, and lasts for 50-100 ms (Church et al., 2019; Gu et al., 2005; Storm, 1989). The source of the mAHP is not fully understood, but it is likely to be caused by the activity of K^+ channels with kinetics that sense voltage and involve slow close rates, such as Kv7 channels, or Ca^{2+} activated K^+ channels, with intracellular calcium influx during the action potential activating the channel (Church et al., 2019; Gu et al., 2005; Niday & Bean, 2021; Storm, 1989). Overall, these results are consistent with the idea that the AHP can represent a negative feedback mechanism, as a single sensor (voltage or Ca^{2+}) may engage these processes to regulate activity.

Structure and mechanism of Kv7 channels

Results presented in this thesis involve regulation of neuronal firing by the K^+ channel, Kv7. Therefore, a brief description Kv7 is warranted. Kv7 channels are voltage-activated K^+ channels that generate a current that activates at voltages below firing threshold. They have slow open (activation) and close (deactivation) kinetics and do not show voltage-dependent inactivation (Brown & Passmore, 2009; Cooper, 2011; Delmas & Brown, 2005; Dwivedi & Bhalla, 2021; Greene & Hoshi, 2017). Kv7 channels are encoded by the *KCNQ* genes , KCNQ2, KCNQ3, and KCNQ5, from which tetramers and can be either hometetramers or heterotetramers (Brown & Passmore, 2009; Cooper, 2011). The heterotetramer formed by KCNQ2/KCNQ3 subunits makes up the majority of the Kv7 channels in the brain while the homotetramer made from KCNQ1 subunits are the main Kv7 channels in cardiac myocytes

(Brown & Passmore, 2009; Dwivedi & Bhalla, 2021; Greene et al., 2017). In rodents, Kv7 channels are localized to the axon initial segment (AIS) and dendritic regions where they are incredibly stable during their baseline activity state, which may include silence, phasic firing of action potentials, or tonic firing of action potentials (Cooper, 2011; George et al., 2009). However, in certain situations Kv7 channels or channel subunits are trafficked to the plasma membrane and can be seen moving during periods of intense loading of the excitatory neurotransmitter glutamate (Dwivedi & Bhalla, 2021). During intense period of neuronal stimulation, Kv7 channels are removed from the membrane via endocytosis, along with the Na^+ channels responsible for propagating the action potential (Dwivedi & Bhalla, 2021). This movement of channels is thought to be neuroprotective (Dwivedi & Bhalla, 2021). Moreover, following activation of muscarinic acetylcholine receptors (mAchRs), KCNQ2 subunits are trafficked to the plasma membrane to aid in recovery of the Kv7 channel current and prevent any large increase in cell excitability (Jiang et al., 2015). Kv7 channels take approximately 100-300 milliseconds to activate, are open at resting membrane voltages, can remain open for long periods of time, and deactivate in approximately 100-450 milliseconds (Brown & Passmore, 2009). Differences in channel activation/deactivation are due to the composition of the Kv7 channel (Brown & Passmore, 2009). Kv7 channels also have a Ca^{2+} sensing domain, which binds the protein calmodulin, CaM (Dwivedi & Bhalla, 2021). When CaM binds Ca^{2+}, this causes a conformational change that lowers the phosphatidylinositol 4,5 bisphosphate (PIP_2) binding affinity of the Kv7 channel and inhibits the activity of the channel as a result (Dwivedi & Bhalla, 2021). Kv7 channels can only bind one CaM and the location of CaM determines the effect of increased Ca^{2+} on channel activity (Dwivedi & Bhalla, 2021). In Kv7.2-7.5 channels, if CaM is bound to the A and B helices, then binding of Ca^{2+} to CaM will cause the channel to close (Dwivedi & Bhalla, 2021). In Kv7.1 channels, the binding of CaM to the channel is competitive with the PIP_2 binding site and can mimic the effects of PIP_2 when PIP_2 levels are depleted (Dwivedi & Bhalla, 2021). Regardless of composition, Kv7 channels are responsible for what is

known as the “M-current”, due to its modulation by the neuromodulator *m*uscarine (Brown & Adams, 1980; Brown & Passmore, 2009). The mechanism behind the muscarinic attenuation of the M current remained a mystery, however we now know that muscarine indirectly attenuates the M-current via PIP_2 (Brown & Adams, 1980; Brown & Passmore, 2009). Although PIP_2 is classically known for its role in the IP3 pathway, muscarine increases the hydrolysis of, PIP_2 by increasing the activity of phospholipase C (PLC) (Brown & Passmore, 2009; Hernandez et al., 2008; Rodríguez-Menchaca et al., 2012; J. Zhang et al., 2018).. The mechanism behind muscarine's effect on the M current works because Kv7 channels depend on PIP_2 to enter the open state and pass current (Delmas & Brown, 2005; Hernandez et al., 2008). Kv7 channels bind PIP_2 at the B helix and depletion of PIP_2 or depolarization of the polar head group prevents Kv7 channels from opening (Dwivedi & Bhalla, 2021).

Due to their low threshold for activation, Kv7 channels are key players in the regulation of intrinsic excitability. For instance, Kv7 channels have been found to be responsible for the fast activity-dependent homeostasis (fADH) in striatal output neurons (SONs) in the mouse brain (Cao et al., 2015). The fADH causes the time between bursts of action potentials to become more variable. It also reduces the number of action potentials fired within the burst, which is important to maintaining proper firing of action potentials and constraining excitability (Cao et al., 2015). Further, Kv7 channels have an established role in the regulation of excitability at the axon initial segment and throughout the axon (Benned-Jensen et al., 2016; Brown & Passmore, 2009; Cooper, 2011). The axon is the part of the neuron that conducts the action potential. Once the action potential reaches the end of the axon, known as the axon terminal, the positive voltage of the action potential causes voltage-gated Ca^{2+} channels to open, which lead to the release of neurotransmitters. At the axon initial segment, Kv7 channels control whether the action potential will be propagated by adjusting the action potential threshold at this portion of the axon (Brown & Passmore, 2009; Cooper, 2011; Vervaeke et al., 2006). Kv7 channels have also been found in the Nodes of Ranvier, which are gaps in the

myelin sheath on the axon, along with the Na^+ channels that help propagate the action potential (Cooper, 2011).

Regulation over shorter timescales: The slow Afterhyperpolarization, Part II and S_K Channels

The slow AHP, sAHP, generally occurs after the mAHP and lasts for approximately five to seven seconds after a burst and also has an unclear etiology (Church et al., 2019; Niday & Bean, 2021; Tiwari et al., 2019). The sAHP may be caused by small conductance calcium-activated K^+ channels (S_K channels) combined with the increased activity of the low affinity isoform of the Na^+/K^+ATPase, hereafter referred to as the dynamic Na^+/K^+ATPase (Tiwari et al., 2019). Thus, SK channels sense and respond to intracellular caused by activity, while the Na^+/K^+ATPase senses intracellular Na^+ to regulate neuronal output. S_K channels take approximately five to fifteen milliseconds to activate and about thirty milliseconds to deactivate (Dwivedi & Bhalla, 2021). The variation in activation time can be accounted for by the variation in S_K channel makeup (Dwivedi & Bhalla, 2021). The S_K channels are encoded by the *SK1*, *SK2*, *SK3*, and *SK4* genes (Shmukler et al., 2001). SK1, SK2, and SK3 subunits form tetramers, which can be homotetramers or heterotetramers (Shmukler et al., 2001). The *SK4* gene encodes a channel that is used in excitable, non-neuronal tissues (Shmukler et al., 2001). The makeup of the channel determines its function and S_K channels can be very variable due to alternative splicing (Shmukler et al., 2001). Increased levels of cytosolic Ca^{2+} is necessary for the activation of S_k channels. Cytosolic Ca^{2+} can increase due to the depolarization of the membrane during an action potential, which opens voltage-gated Ca^{2+} channels which allow Ca^{2+} to influx into the cell (Church et al., 2019; Gu et al., 2005; Niday & Bean, 2021; Storm, 1989). Certain excitatory receptors, such as NMDA receptors, also allow Ca^{2+} influx in addition to their main ions (Shrivastava et al., 2020). In a third scenario, activity can stimulate Ca^{2+} release from intracellular stores (Dwivedi & Bhalla, 2021). Despite their reliance on intracellular Ca^{2+}, these channels do not possess an intrinsic Ca^{2+} binding domain (Shmukler et al., 2001).

Rather, S_k channels rely on the protein calmodulin (CaM), which is bound to the channel, to "sense" intracellular Ca^{2+} levels (Shmukler et al., 2001). S_K channels can have variable numbers of CaM bound, with some channels having up to four (one CaM bound to each subunit of the tetramer) (Shmukler et al., 2001). The amount of CaM bound also influences the channel's kinetics and open probability (Shmukler et al., 2001). Binding of Ca^{2+} to CaM opens S_K channels, which lowers the membrane potential of the cell (Shmukler et al., 2001).

Regulation over shorter timescales: The ultraslow afterhyperpolarizations Part III, the $Na^{-}K^{+}$ ATPase

A third AHP, known as the ultra-slow afterhyperpolarization, usAHP, has been identified in the spinal locomotor circuits of *Xenopus* tadpoles and rodents, as well as in Drosophila larvae (Picton et al., 2017; Pulver & Griffith, 2010; Zhang & Sillar, 2012). In contrast to the other AHPs which are largely driven by Ca^{2+}, increases in intracellular Na^{+} activate the dynamic Na^{+}/K^{+}ATPase which has a low affinity for Na^{+}. The Na^{+}/K^{+}ATPases are ion pumps that move two K^{+} ions into the cell and three Na^{+} ions out of the cell using energy from ATP hydrolysis (H.-Y. Zhang & Sillar, 2012). Although commonly known for its role in the constitutive regulation of ions, the low-affinity isoform of the pump only activates when intracellular Na^{+} rises, such as after a burst of action potentials. The imbalance of charge movement (+2 in, +3 out, -1 net) produces a negative current that hyperpolarizes the cell and reduce excitability. Following periods of intense, long activity, the dynamic Na^{+}/K^{+}ATPase turns on and begins to hyperpolarize the membrane to dampen excitability. The usAHP is proposed to regulate excitability on the scale of seconds to a minute by allowing neurons to adjust their future activity based upon their past activity (H.-Y. Zhang & Sillar, 2012). This has been clearly demonstrated in the *Xenopus* tadpole, where the interval between swimming episodes is linearly correlated with the length of the previous swimming episode (H.-Y. Zhang & Sillar, 2012).

Structure of the Na^+/K^+ATPases

The dynamic Na^+/K^+ATPase and other Na^+/K^+ATPases are heterotrimers, as they are constructed from three different subunits (Shrivastava et al., 2020). The α subunit is responsible for the binding and export of Na^+ ions and import of K^+ ions, as well as the binding and hydrolysis of ATP (Shrivastava et al., 2020). The α subunit is made up of 3 domains: the nucleotide-binding domain, the actuator domain, and the phosphorylation domain (Shrivastava et al., 2020). The β subunit modulates both the insertion of the α subunit into the membrane and the activity of the Na^+/K^+ATPase (Shrivastava et al., 2020). The FXYD subunit modulates the affinity for Na^+, K^+, and ATP. There are four different α subunits, three different β subunits, and seven different FXYD subunits which can be combined in any fashion (Shrivastava et al., 2020). The constitutively active Na^+/K^+ATPase responsible for baseline ion regulation contains the α1 subunit which endows it with a higher affinity for Na^+ ions. In contrast, the dynamic Na^+/K^+ATPase contains the α3 subunit with a lower affinity for Na^+ ions (Shrivastava et al., 2020). The dynamic Na^+/K^+ATPase is only expressed in neurons while the housekeeper Na^+/K^+ATPase is ubiquitously expressed (Shrivastava et al., 2020). As for the β and FXYD subunits, all three β subunits are expressed in the brain and FXYD1, 6, and 7 are expressed in the brain (Shrivastava et al., 2020). However, it is unclear which β and FXYD subunit the dynamic and housekeeper Na^+/K^+ATPases contain. Astrocytes, which are specialized cells in the brain that provide metabolic and regulatory support, express Na^+/K^+ATPases that utilize the α2 subunit, hereafter referred to as the astrocytic Na^+/K^+ATPase, and this subunit has a higher affinity for K^+ ions and aids in clearance of extra K^+ ions from the extracellular space following periods of intense neuronal activity (Shrivastava et al., 2020). In this way, the dynamic Na^+/K^+ATPase and the astrocytic Na^+/K^+ATPase work together to rebalance the electrochemical gradients of Na^+ and K^+ following periods of high neuronal excitation. Na^+/K^+ATPases with the α4 subunit exist but are not relevant for this study (Shrivastava et al., 2020)

What about continuous behaviors?

Previous work has established a role for the dynamic Na^+/K^+ATPase in the regulation of intrinsic excitability (Hachoumi et al., 2022; Picton, Zhang, et al., 2017; H.-Y. Zhang & Sillar, 2012). However, all work on the usAHP and the role of the dynamic Na^+/K^+ATPase in intrinsic excitability regulation has been done in locomotor circuits. These circuits produce movements that are intermittent like swimming or crawling, where there is a pause in between active periods (Picton, Zhang, et al., 2017; H.-Y. Zhang & Sillar, 2012). This pause is variable, and the length of the break is usually correlated with the length of the active period (H.-Y. Zhang & Sillar, 2012). However, there is a glaring gap in our knowledge of how the dynamic Na^+/K^+ATPase regulates intrinsic excitability in neurons that produce continuous behaviors. This begs the question: what role does the dynamic Na^+/K^+ATPase play in the regulation of intrinsic excitability for neurons that generate continuous behaviors? For neurons in circuits that produce continuous behaviors, the active period may not come with a "break", or this break is very short and non-variable. In order to answer this question, we will investigate the role of the dynamic Na^+/K^+ATPase in the neurons that innervate the respiratory muscles in the American Bullfrog.

Background on the study system

Unlike humans, frogs ventilate the lungs using positive pressure, as they force air into their lungs rather than creating a vacuum that “pulls” air into them (Kogo et al., 1994; Kogo & Remmers, 1994). Frogs use four major muscles to breathe: the buccal elevators, the buccal depressors, the glottal dilators, and the glottal constrictors (Kogo et al., 1994). We previously referred to the buccal elevators/depressors as the respiratory pump muscles and the glottal dilators/constrictors as the respiratory valve muscles (Kogo & Remmers, 1994). The neurons that innervate the buccal elevators/depressors are known as hypoglossal motoneurons and those that innervate the glottal dilators/constrictors are known as vagal motoneurons (Kogo & Remmers, 1994). These are the two populations of motoneurons that will be used in this study.

Overall, our major goal was to define fast activity-dependent feedback for the control of rhythmic, continuous behaviors.

CHAPTER II: FIRING RATE HOMEOSTASIS THROUGH THE CO-EXPRESSION OF TWO FEEDBACK MECHANISMS THAT DETECT SEPARATE ASPECTS OF NEURONAL ACTIVITY

Methods

Housing and Animal Care

All experiments performed were approved by the Institutional Animal Care and Use Committee (IACUC) at UNC-Greensboro. Adult American Bullfrogs, *Lithobates catesbeianus*, were purchased from Rana Ranch (Twin Falls, Idaho) and were housed in 20-gallon dechlorinated and enriched tanks bubbled continuously with room air with access to both wet and dry areas. Frogs were maintained on a 12-hour light/dark cycle and fed once per week. Water was cleaned daily and changed as needed. All experiments occurred during the light cycle.

Preparation of brainstem slices

Frogs were anesthetized with 1 mL isoflurane in a ~1 L container until loss of the toe-pinch reflex. Euthanasia was achieved via rapid decapitation. Brainstem dissection was performed in ice-cold artificial cerebrospinal fluid (aCSF) bubbled with 98.5% O_2/1.5% CO_2 where the forebrain, optic tectum, brainstem, and spinal cord were removed from the head. The forebrain was crushed, the spinal cord was trimmed, and the brainstem was transferred to a small, Sylgard-coated Petri dish for dye-loading. The brainstem preparation was stabilized by the addition of two pins, one in the rostral midbrain and one in the spinal cord.

To identify vagal and hypoglossal motoneurons, neurons were backfilled through their axons with a fluorescent dye (Dextran, Tetramethylrhodamine, 3000 MW, anionic) through their axons using standard methods (Zubov et al., 2021).

Transverse 300 µm slices of the brainstem region were cut using a Vibratome Series 1000 sectioning system in ice-cold aCSF bubbled with 98.5% O_2/1.5% CO_2. To further ensure that the motoneurons used in this study were those innervating the glottal dilator and buccal

floor muscles, only slices that were approximately 300 µm caudal to the obex to approximately 1200 µm rostral to the obex were used. This region has previously been shown to house motoneurons, where ~75% receive respiratory-related synaptic input (Amaral-Silva & Santin, 2022) . Slices were kept in room temperature aCSF bubbled with 98.5% O_2/1.5% CO_2 throughout the experiments.

Solutions

Frog aCSF was made with the following reagents in the following concentrations (in mM): 104 NaCl, 4 KCl, 1.4 $MgCl_2$, 7.5 Glucose, 1 $NaHPO_4$, 40 $NaHCO_3$, 2.5 $CaCl_2$.

Intracellular solution was made with the following reagents in the following concentrations (in mM): 110 K-gluconate, 2 $MgCl_2$, 10 HEPES, 1 Na_2ATP, 0.1 Na_2GTP, 2.5 EGTA.

Cadmium was used at a concentration of 30 µM. Cadmium chloride was purchased from Fisher Scientific and was added to pre-made aCSF on the day of experiments.

Ouabain was purchased from HelloBio, made into 10 mM stocks in ddH_2O and frozen until use. Ouabain was used at a concentration of 2 µM or 20 µM.

XE991 was purchased from HelloBio, made into 100 mM stocks in ddH_2O and frozen until use. XE991 was used at a concentration of 10 µM.

Dextran, Tetramethylrhodamine, 3000 MW, anionic was purchased from Fisher Scientific, reconstituted in PBS, aliquoted, and frozen until use.

Aliquots did not undergo any freeze/thaw cycles. All thawed aliquots were discarded at the end of the day. The exception to this rule was Dextran, Tetramethylrhodamine, 3000 MW, anionic, where aliquots did undergo freeze/thaw until empty. Freeze/thaw cycles did not appear to have any negative effects on this reagent.

Electrophysiology

Current clamp experiments

Current clamp experiments were performed on both the 200B amplifier (Molecular Devices) or the 700A amplifier (Molecular Devices). Patch pipettes for electrophysiological recordings were pulled on a P-87 Puller (Sutter Instruments) with a tip resistance between 2.5-5 MΩ and filled with intracellular solution. Glass used for patch pipettes was purchased from either Harvard Apparatus (1.5 ODx1.17IDx100L mm) or World Precision Instruments (1.5ODx1.12ID). Only cells that were positive for fluorescence were used, as these are neurons that innervate respiratory muscles. Cells were given between two and three minutes to recover after obtaining whole-cell access. Cells with depolarized membrane potentials (approximately -25mV non-spiking) were discarded. Membrane potential was held at -55mV in current clamp mode by injecting a bias current. Neurons were initially injected with a range of currents to estimate maximal sustaining firing frequency. When cells entered depolarization block, current was reduced to obtain spiking through a 10 second pulse. Maximum current injected was 1 nA in this study. Following the 10 second stimulation period, each cell was given approximately seventy-five seconds of recovery with input resistance measurements every 10 seconds. The protocol is further demonstrated in Figure 1 below. Following the initial usAHP measurement, 2 µM ouabain/10 µM XE991/30 µM Cd^{2+} was washed in for 15 minutes. The protocol was rerun at five-minute intervals and the cell was held at -55mV.

To determine the physiological roles of the ion transporters identified in this study, a protocol was constructed that simulated the real physiological synaptic input that vagal motoneurons receive to generate breathing. Our lab has recently developed a semi-intact preparation that allows simultaneous access to extracellular nerve root recordings and motoneuron patch clamp recordings during the ongoing respiratory rhythm (Amaral-Silva & Santin, 2022) (Figure 7A). Direct recordings of synaptic currents associated with breathing

obtaining from the semi-intact preparation allowed us to simulate synaptic input that vagal motoneurons received during respiratory bursts (Fig 7A). For this, we constructed a current clamp protocol that injected cells with current that matched the exact waveform of synaptic input recorded from the intact network and paced them at a frequency consistent with the respiratory rhythm, we termed this protocol the “physiological protocol”. Thus, we could restore breathing motor patterns in neurons completely disconnected from the network. (Amaral-Silva & Santin, 2022; Vallejo et al., 2018) (Fig 7A). Bursts from the physiological protocol were qualitatively similar to those receiving real synaptic inputs in the intact network (Fig 7A, qualitative observations). The physiological protocol was designed by Dr. Michael Gray, with data gathered by Amaral-Silva, L. The protocol consisted of ten, approximately one-second physiologically relevant stimulations separated by an approximately nine-second-long interval. Cells were allowed the same recovery period after whole-cell access was obtained. Cells were held at -55mV in current clamp mode. The baseline measurement was taken five minutes after the cell was put through the physiological protocol continuously. Only neurons that could be controlled by the bias current were included in these experiments. After the baseline measurement, 2 µM ouabain was washed in for fifteen minutes followed by 10 µM XE991 mixed with 2 µM ouabain wash-in for fifteen minutes (Figure 2). The physiological protocol was run continuously during all drug wash-ins and V_m measurements were taken at the beginning, five-minute, ten-minute, and fifteen-minute time points (Figure 2). V_m measurements represent the average V_m for that minute. The usAHP was evoked before the baseline measurement and after the XE991 wash-in.

Figure 1: Current Clamp Experiment Protocols:

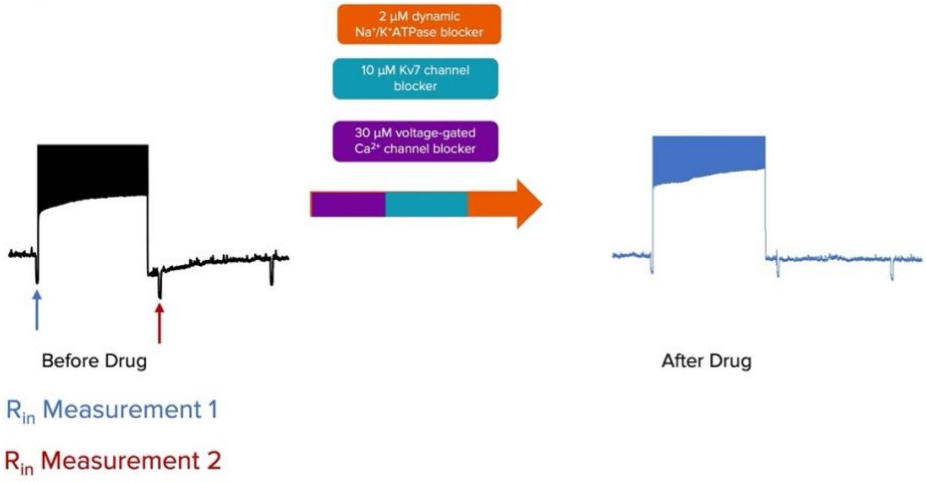

To determine the ionic basis of the usAHP, the usAHP was evoked in the presence of three pharmacological agents (separate applications). Here, the protocol for the dynamic Na^+/K^+ATPase blocker ouabain application is shown. The usAHP was evoked prior to wash-in and input resistance (R_{in}) was measured before and after stimulation, as well as throughout the after-stimulation recovery period. Input resistance is inversely related to membrane conductance, which is a measure of how leaky the cell is. Lower R_{in} (smaller dip) corresponds to high conductance (very leaky) and vice versa. This same protocol was used for the Kv7 channel blocker XE991 and the voltage-gated Ca^{2+} channel blocker Cd^{2+}.

Figure 2: Physiological Protocol

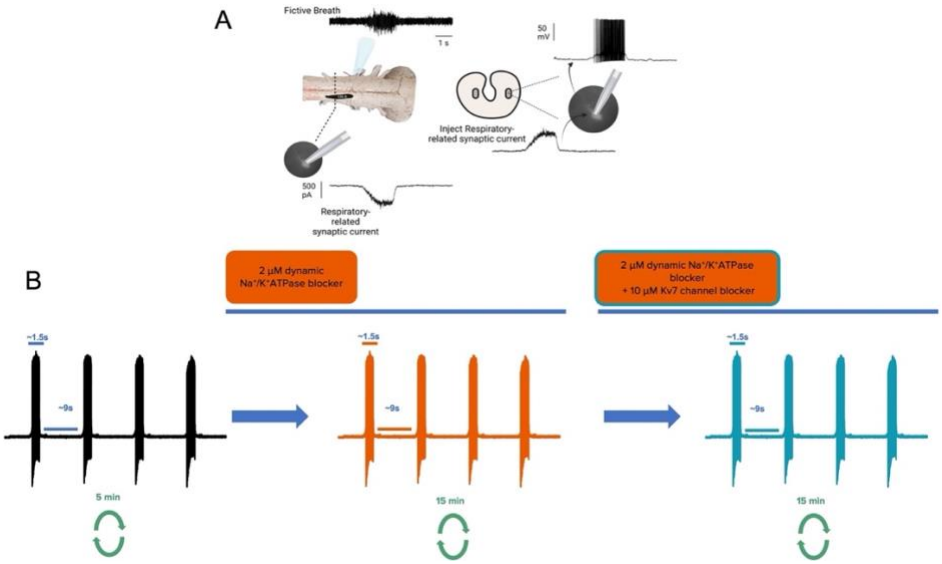

(A) To determine the physiological role of the dynamic Na^+/K^+ATPase and Kv7 channels, we designed a protocol that would allow us to inject current that exactly matches the synaptic input received by vagal motoneurons during a fictive breath. We used data from the semi-intact preparation developed by Amaral-Silva, L that allowed us to gain knowledge of synaptic input received by vagal motoneurons during a fictive breath (Amaral-Silva & Santin, 2022). **(B)** Dr. Michael Gray was able to take the synaptic input and turn this into a protocol that injected the same amount of current in the same waveform at physiologically relevant intervals. To use this protocol, we first acclimated cells to the activity by continuously running the protocol for five minutes in normal aCSF. Then, to determine the role of the dynamic Na^+/K^+ATPase, we washed in the dynamic Na^+/K^+ATPase blocker, ouabain for fifteen minutes while the protocol ran continuously (orange). Lastly, we washed in the Kv7 channel blocker XE991 for fifteen minutes to determine the role of Kv7 channels (blue).

Voltage clamp experiments

All voltage clamp experiments were performed on the 200B amplifier (Molecular Devices). Patch pipettes were pulled using the P-87 puller with a tip resistance between 2.5-4 MΩ using the same glass as the current clamp experiments. Tips were wrapped in Parafilm to reduce pipette capacitance and filled with intracellular solution. Cells were given one minute to recover following establishment of whole-cell access. Series resistance was compensated between 75-98% and only cells with an effective series resistance of 3 MΩ or lower with a change of less than 0.5 MΩ were used in this study. The outward K^+ current was then evoked with a step protocol that moved from -68mV to +12mV in 10 mV increments. After the initial outward K^+ current was determined, XE991 (10 μM) was washed in for five-ten minutes. Figure 3 shows the protocol used. The Kv7 channel current density was determined by taking the difference between the outward K^+ current in aCSF and the outward K^+ current after wash-in of XE991, normalized for cell capacitance.

Figure 3: Voltage Clamp Protocol

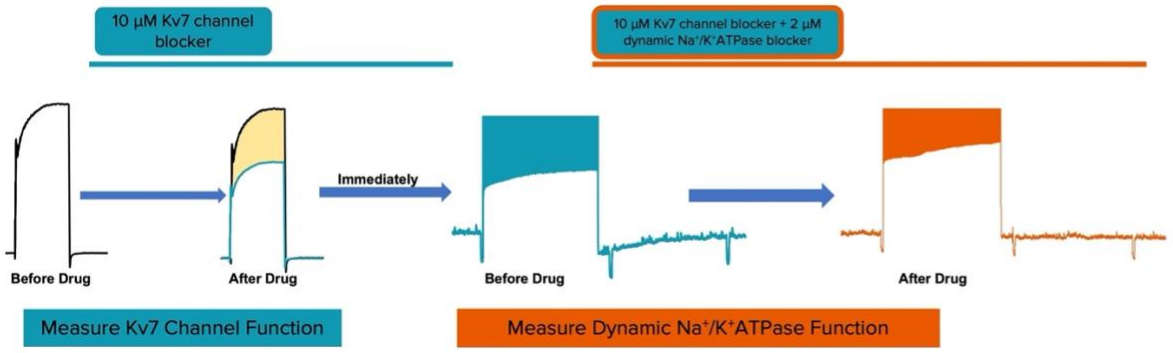

To determine the functional relationship between the dynamic Na^+/K^+ATPase and Kv7 channels, the outward K^+ current was evoked in voltage clamp (far left, black). The Kv7 current portion of the outward K^+ current was determined using the Kv7 channel blocker XE991 (left, blue). The Kv7 current (yellow) was found by subtracting the XE991 trace (blue) from the control trace (black). The Kv7 channel current was normalized for cell capacitance to determine the Kv7 channel density in the cell. To establish the contribution of the dynamic Na^+/K^+ATPase to the usAHP, the usAHP was evoked in the presence of XE991 (middle, blue) and in the presence of XE991 and the dynamic Na^+/K^+ATPase blocker, ouabain (far right, orange). The difference between the usAHP in XE991 (blue) and XE991+Ouabain (orange) was used to determine the Na^+/K^+ATPase role in the usAHP.

Statistics and Data Analysis

Data analysis was performed in Excel using ClampFit and LabChart. Statistics were performed in GraphPad (Prism). Correlations were determined using the Pearson correlation tests. To determine significance between groups, the one-way ANOVA with Holm Sidak comparison test and unpaired T. tests were run.

Results

Characterization of the usAHP in two populations of respiratory neurons

Motoneurons can regulate firing rate on the time scale of several seconds through negative feedback that involves activation of the Na^+/K^+ATPase by intracellular Na^+. Accordingly, intense neuronal firing evokes an ultraslow afterhyperpolarization (usAHP) that lasts for 10-60 s to reduce membrane excitability. Because activation of an ion pump generates current flow through the translocation of ions, the usAHP is not associated with changes in the membrane input resistance (R_{in}) as would occur if an ion channel was opening or closing (Hachoumi et al., 2022; Picton, Nascimento, et al., 2017; H.-Y. Zhang et al., 2015; H.-Y. Zhang & Sillar, 2012). We assessed the presence of activity-dependent usAHP in identified motoneurons that gate airflow into the lung to regulate breathing in American bullfrogs (vagal; Figure 4A). Following 10 s of near-maximal action potential firing, vagal motoneurons exhibited an usAHP that that lasted between 10-60 s and ranged between ~4-12 mV (Fig. 4B), like that observed in locomotor neurons (H.-Y. Zhang & Sillar, 2012). We did not observe an usAHP in hypoglossal motoneurons (*N*=14, average usAHP amplitude=3.14 mV). Therefore, we ended our investigation in hypoglossal motoneurons and continued with only vagal motoneurons. To our surprise, unlike the classic pump-dependent usAHP in locomotor neurons, we found that the usAHP was associated with decreases in R_{in} that recovered in tandem with the membrane potential following stimulation (Fig 4E). Interestingly, the drop in R_{in} following stimulation was variable from cell to cell, ranging from roughly no change to a 40% reduction (Fig 4C-D). We did not observe a correlation between the amplitude or the rate of recovery of the usAHP with the reduction in R_{in} (Fig 4F-G), suggesting that a “similar” usAHP is generated across neurons through multiple mechanisms. In support of this assertion, neurons that had small-to-no decreases in R_{in} had an usAHP triggered by spiking, as block of action potentials during strongly reduced the usAHP (Fig 4H, J). In contrast, neurons with the largest decreases in R_{in} retain their usAHP following block of action potential during stimulation (Fig 4I-J). Therefore, two

mechanisms—one that depends on spiking and does not alter R_{in} and one that depends either on depolarization or Ca^{2+} influx and reduces R_{in} —feedback to reduce excitability in following stimulation in the same population of identified neurons.

Figure 4: The usAHP in Vagal Motoneurons

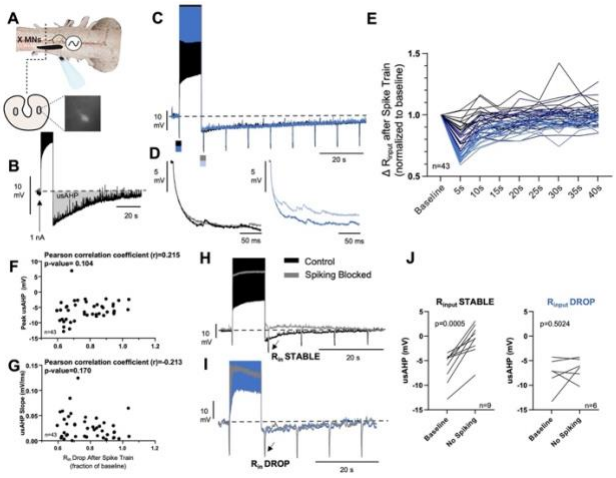

(A) Motoneurons in the vagal motor pool were used for this study and identified by backfilling their axons with fluorescent dye before the brainstem was sliced into transverse slices. **(B)** Representative usAHP following a 1 nA current injection to generate maximal action potential firing. **(C)** Representative usAHP traces with input resistance (R_{input}/R_{in}) checks before stimulation and during the after-stimulation recovery period. We noticed a drop in R_{in} in some cells following stimulation and termed this the "R_{in} Drop". **(D)** R_{in} measurements before and after stimulation in two cells: one with stable R_{in} (black and grey) and one with the R_{in} Drop (blue). **(E)** R_{in} measurements over time for cells with stable R_{in} (black) and the R_{in} Drop (blue). The R_{in} for cells with an R_{in} Drop recovered back to baseline throughout the recovery period (5s to 40s). **(F)** The R_{in} Drop is not correlated with the amplitude of the usAHP (Pearson correlation coefficient=0.215, *P*=0.104). **(G)** The R_{in} Drop is not correlated with the duration of the usAHP (Pearson correlation coefficient= -0.213, *P*=0.170. **(H)** Cells with stable R_{in} lose their usAHP when spiking is blocked (grey). **(I)** Cells with the R_{in} Drop keep their usAHP after spiking has been blocked (grey). **(J)** Amplitude of the usAHP before and after spiking was blocked. Amplitude of the usAHP was nearly 0 in cells with stable R_{in} after spiking was blocked. Cells with the R_{in} Drop exhibited a variety of responses to spiking blocked.

Identifying the ion transporters responsible for generating the usAHP

To determine the ionic basis of the usAHP we observed, we blocked candidate mechanisms that might underlie the usAHP. We chose to focus on the dynamic Na^+/K^+ATPase first, as it has already been implicated in the usAHP in amphibians and rodents (Hachoumi et al., 2022; Picton, Zhang, et al., 2017; H.-Y. Zhang & Sillar, 2012). Therefore, we first employed the dynamic Na^+/K^+ATPase blocker, 2 μM ouabain. We found that ouabain blocked the usAHP variably and block of the usAHP by ouabain was inversely correlated with the R_{in} Drop (Figure 5A, E). Differential sensitivity to ouabain and its relationship to changes in the membrane conductance following stimulation led us to hypothesize that maximal stimulation was leading to the opening of a channel. A number of channels could be responsible for decreasing R_{in} and lowering the membrane potential (Dunn & Kaczorowski, 2019; Dwivedi & Bhalla, 2021; Vatanparast & Janahmadi, 2009). We hypothesized that a K^+ channel was also responding to activity in our system as these channels have been implicated in other aspects of activity dependent intrinsic excitability regulation and explain the reduction in R_{in}. Several K^+ channels sense variables related to activity, including Ca^{2+}, Na^+, and membrane depolarization (Cao et al., 2015; Dwivedi & Bhalla, 2021; Vatanparast & Janahmadi, 2009). We quickly ruled out the possibility of a Na^+-sensitive K^+ channel due to the results of our no spiking experiments in Figure 4. Therefore, we hypothesized that the usAHP was caused by the activity-dependent activation of either a Ca^{2+}-activated K^+ channels or voltage-sensitive K^+ channel Kv7 due to their implication in the regulation of intrinsic excitability on similar time scales as we are studying (Cao et al., 2015; Chen et al., 2011; Church et al., 2019; Cooper, 2011; Dwivedi & Bhalla, 2021; Storm, 1989; Vatanparast & Janahmadi, 2009; Vervaeke et al., 2006). To investigate whether Kv7 or Ca^{2+} activated K^+ channels were involved in the usAHP, we evoked the usAHP in the presence of 30 μM Cd^{2+} to block voltage-gated Ca^{2+} channels thus preventing activation of Ca^{2+} activated K^+ channels or 10 μM XE991, a blocker of Kv7 channels (Golowasch et al., 1999;

Greene et al., 2017). Our results showed that Cd^{2+} had no effect on the amplitude of the usAHP or the value of the R_{in} drop and there was no significant correlation between block of the usAHP and reduction in R_{in} Drop (*N*=14) (Pearson correlation= -0.1598, *P*=0.5857) (Fig 5A-C, G). Meanwhile, treatment with XE991 significantly reduced the amplitude of the usAHP compared with Cd^{2+}, while also increasing the value of the R_{in} drop by increasing the second R_{in} measurement (*N*=18) (one way ANOVA with Holm Sidak comparison test, *P*=0.035) (Fig 5A-C,F). We found that reduction of the usAHP and R_{in} drop were significantly negatively correlated (Pearson correlation=-0.6808, *P*=0.0026) (Fig 5F). Therefore, we concluded that Kv7 channels are partially responsible for the usAHP. Based on the results of the Cd^{2+} experiments, we were also able to conclude that Kv7 is activated in vagal motoneurons by sensing the voltage of the membrane and not impacted by Ca^{2+} sensing. The identification of Kv7 as the second contributor to the usAHP was surprising, as the interaction between an ion pump and a channel has not yet been studied in the context of the regulation of intrinsic excitability. This led us to test how these two ion transporters were interacting functionally to maintain the cell's intrinsic excitability.

Figure 5: The Dynamic Na^+/K^+ATPase and Kv7 channels Are Responsible for the usAHP

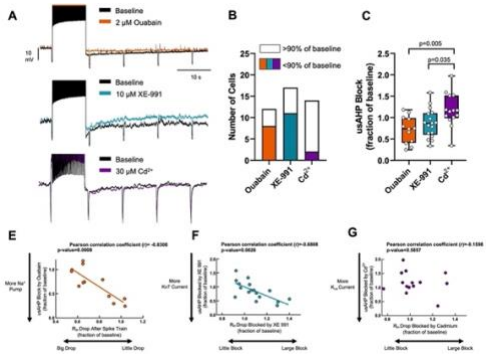

(A) Representative traces of each drug treatment: ouabain (top, orange, dynamic Na^+/K^+ATPase blocker), XE991 (middle, blue, Kv7 channel blocker), and Cd^{2+} (bottom, purple, voltage-gated Ca^{2+} channel blocker). While treatment with ouabain and XE991 reduced the amplitude of the usAHP, treatment with Cd^{2+} did not. **(B)** Quantification of cells that responded to ouabain, XE991, and Cd^{2+}. Colored portions of the bars indicate cells where the usAHP was blocked. Uncolored parts of the bars represent cells where it was not. **(C)** Average responses to ouabain, XE991, and Cd^{2+} showed that Cd^{2+} had a significantly smaller usAHP block than either ouabain (*P*=0.005) or XE991 (*P*=0.035) as determined by a one-way ANOVA with the Holm Sidak comparison test. **(E)** Blockade of the usAHP is significantly inversely correlated with the R_{in} Drop (Pearson correlation coefficient= -0.8308, *P*=0.0008). Block of the usAHP is represented as fraction of baseline, where the amplitude of the usAHP in ouabain is divided by the amplitude in normal aCSF. The R_{in} Drop was calculated by dividing the first R_{in} measurement after stimulation by the R_{in} measurement taken before stimulation. Here, the dynamic Na^+/K^+ATPase is referred to as the Na^+ pump. **(F)** Block of the usAHP by XE991 was significantly inversely correlated to block of the R_{in} Drop (Pearson correlation coefficient= -0.6808, *P*=0.0026). R_{in} Drop block was calculated by dividing the R_{in} Drop from the XE991 treatment by the R_{in} Drop in normal aCSF. **(G)** Treatment with Cd^{2+} was ineffective, thus no correlation was seen between block of the usAHP and block of the R_{in} Drop (Pearson correlation coefficient= -0.1598, *P*=0.5857).

Quantifying the Relationship between the Kv7 channel current and the dynamic Na^+/K^+ATPase at the functional level

Our previous experiments suggested that neurons that use the dynamic Na^+/K^+ATPase to regulate excitability rely less on Kv7 and vice versa. Therefore, we sought to determine the functional relationship between the Kv7 channels and the dynamic Na^+/K^+ATPase on a cell-by-cell basis. Therefore, we performed voltage clamp experiments to determine the density of the Kv7 current in each cell (a functional assessment of channel activity), followed by evoking the usAHP in XE991 and in XE991 combined with ouabain (see Figure in methods for protocol). The contribution of the dynamic Na^+/K^+ATPase was then determined by comparing the usAHP amplitude in XE991 and in XE991 combined with ouabain. We found that neurons with larger Kv7 current densities generally had smaller responses to ouabain, and those with smaller Kv7 current densities had progressively larger sensitivity to ouabain (*N*=16) (Fig 6A-C). Therefore, on the functional level, the Kv7 current and the dynamic Na^+/K^+ATPase appear to be inversely correlated. Interesting, although this relationship was not linear, with a steeper slope in the bottom ~80th percentile and a shallower slope in the upper ~20th percentile (Fig 6A). Altogether these results indicate that there is an inverse functional relationship between Kv7 and the dynamic Na^+/K^+ATPase, which contributes to activity-dependent feedback across a population of respiratory motoneurons.

Figure 6: The Functional Relationship Between the Dynamic Na^+/K^+ATPase and Kv7 channels

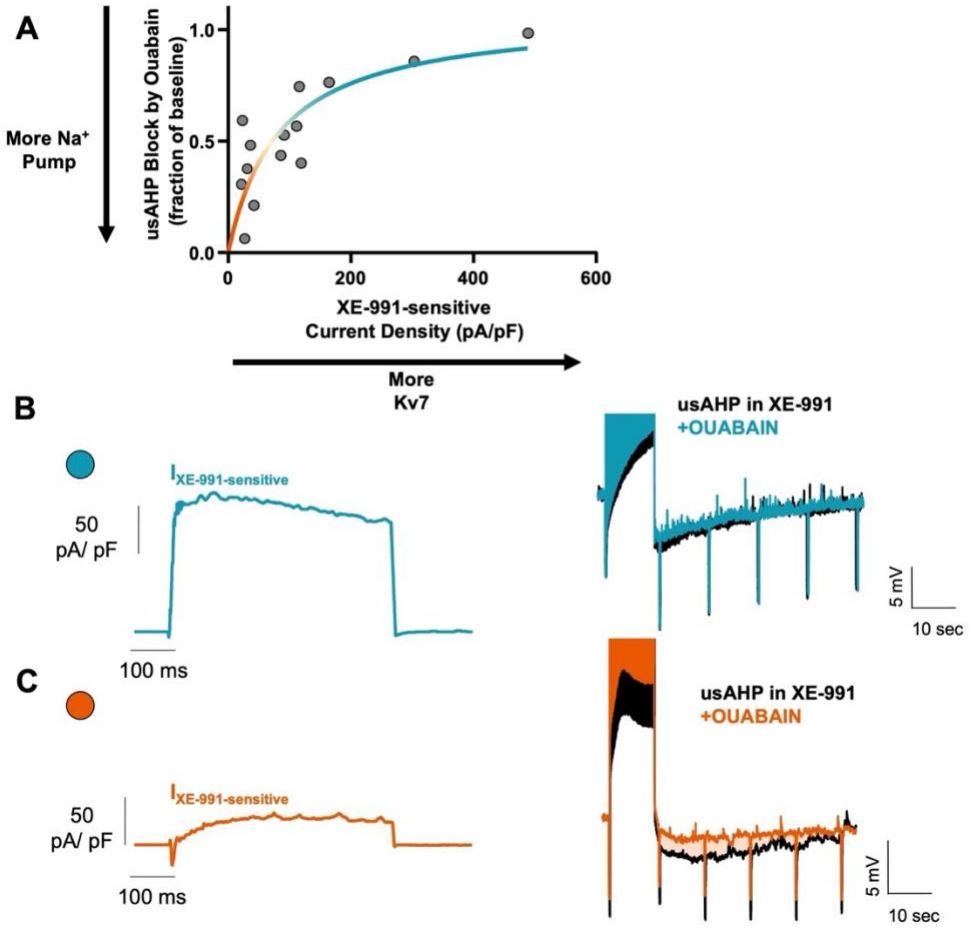

(A) There was an inverse correlation between the XE991 sensitive current channel density (Kv7 channel density) and usAHP block by ouabain (dynamic Na^+/K^+ATPase blocker). Here, as in Figure 5, the dynamic Na^+/K^+ATPase is referred to as the Na^+ pump. **(B)** Cells with large XE991 sensitive currents have little to no response of the usAHP to ouabain. **(C)** Cells with small XE991 sensitive currents have a sizable response to ouabain.

Kv7 channels and the dynamic Na^+/K^+ATPase interact to control physiological firing rates

While intense neuronal stimulation is one way to test for the presence of the dynamic Na^+/K^+ATPase, these (and most neurons) do not receive maximal, long stimuli. Rather, respiratory motoneurons in the Bullfrog receive ~1 s bursts of synaptic input every 6-10 seconds (Vallejo et al., 2018). Therefore, a protocol was constructed that simulated the real physiological synaptic input that vagal motoneurons receive to generate breathing. Our lab has recently developed a semi-intact preparation that allows simultaneous access to extracellular nerve root recordings and motoneuron patch clamp recordings during the ongoing respiratory rhythm (Amaral-Silva & Santin, 2022) (Figure 7A). Direct recordings of synaptic currents associated with breathing obtaining from the semi-intact preparation allowed us to simulate synaptic input that vagal motoneurons received during respiratory bursts (Fig 7A). For this, we constructed a current clamp protocol that injected cells with current that matched the exact waveform of synaptic input recorded from the intact network and paced them at a frequency consistent with the respiratory rhythm. Thus, we could restore breathing motor patterns in neurons completely disconnected from their normal networks (Fig 7A). We found that average firing frequency during the bursts rose with the application of both drugs; however, the response to each drug appeared to be inversely correlated (*N*=16) (Fig 7B-C). That is, in cells where ouabain strongly enhanced firing rate, those neurons had smaller responses to XE991. Neurons with dramatic responses to XE991 had little-to-no responses to ouabain (Fig 7C). Therefore, neurons appear to use different combinations of the dynamic Na^+ pump and Kv7 to regulate firing rates through activity-dependent feedback.

Figure 7: The Physiological Role of the Dynamic Na^+/K^+ATPase and Kv7 channels

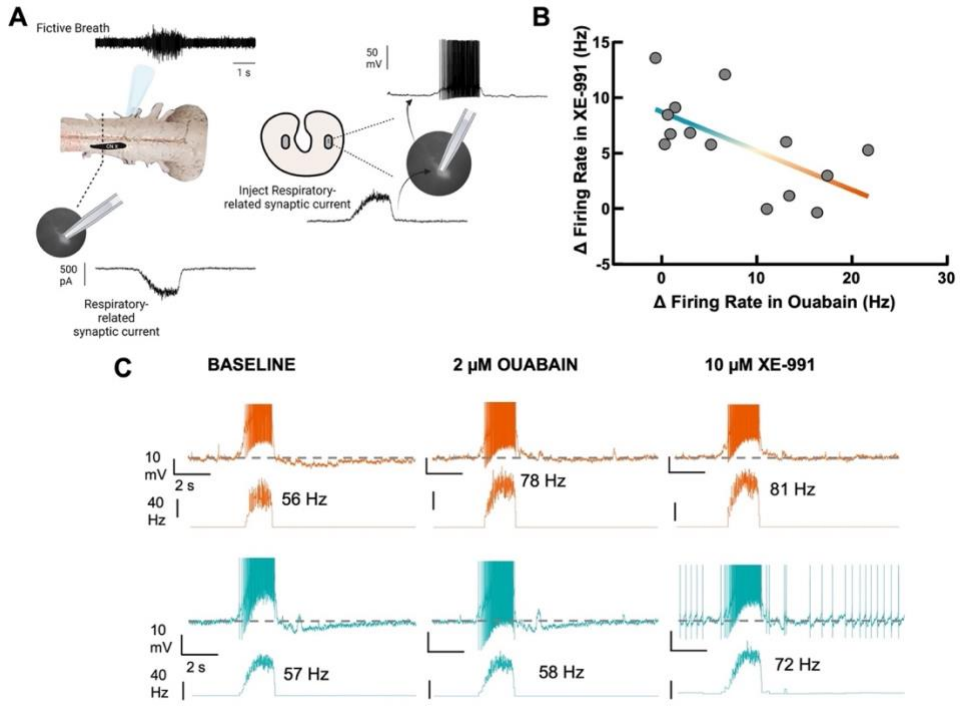

(A) To create the protocol used to determine the physiological role of the dynamic Na^+/K^+ATPase, the semi-intact preparation was used to collect data on the synaptic input (respiratory related synaptic current) received by cells that fired action potentials during the fictive breath. The respiratory related synaptic current was then injected into isolated motoneurons in slices of the brainstem to produce bursts of action potentials that were qualitatively similar to those seen in the intact preparation. **(B)** The dynamic Na^+/K^+ATPase and Kv7 channels are inversely regulate excitability during physiological activity. This is inferred from the response of cells to ouabain and XE991. Cells with large responses to ouabain had smaller responses to XE991 and vice versa. Some cells had similar responses to both drugs (middle of line). **(C)** Representative traces of cells that responded dramatically to ouabain (orange, top) or XE991 (blue, bottom). The top trace of each pair is the original trace, and the bottom trace is the frequency.

Confirming the Activity Dependent Nature of Regulation by the Dynamic Na^+/K^+ ATPase and Kv7 Channels

The previous experiment suggests that the Na^+ pump and Kv7 regulate firing rate through activity-dependent feedback. In order to determine whether these mechanisms were truly working through activity-dependent feedback, rather than actions on the membrane potential independent of activity, we sequentially applied ouabain and XE991 to cells that were silent in current clamp mode and measured changes to resting membrane potential throughout a fifteen-minute wash-in period for each drug (fifteen minutes for each drug, thirty-minute total). In support of the actions of these drugs disrupting activity-dependent regulation of firing, we saw observed little-to-no change to resting membrane potential with either drug at the concentrations we used throughout this study and no significant difference between changes in membrane potential between ouabain and XE991 treatments (*N*=10) (Figure 8). Moreover, when the usAHP was evoked following application of both drugs, it was largely diminished (unpublished observation). Therefore, Kv7 and the dynamic Na^+/K^+ATPase are acting in an activity dependent manner to constrain activity within a tight range.

Figure 8: The Activity Dependent Nature of the Dynamic Na^+/K^+ATPase and Kv7 Channels

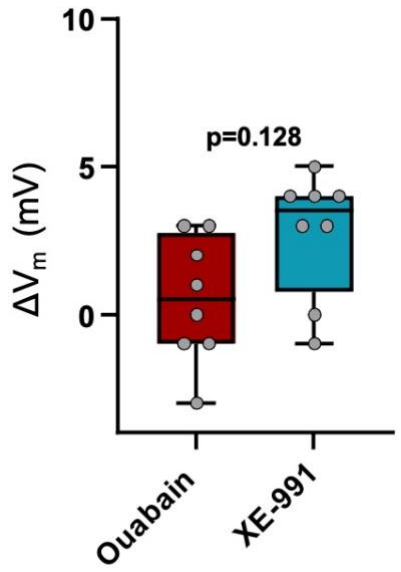

When ouabain and XE991 (separate applications) were applied to cells where action potential generation was prevented (no activity), little to no change in resting membrane potential (V_m) was observed. On average, there was no significant difference between change in V_m following XE991 treatment when compared with ouabain treatment as determined by an unpaired T test (*P*=0.128).

To further confirm that our dose of ouabain was targeting only the dynamic Na^+/K^+ATPase and not also targeting the housekeeper Na^+/K^+ATPase, we applied 20 μM ouabain to cells that were silent in current clamp mode and monitored resting membrane potential. In each trial, application of the higher dose of ouabain led to a dramatic rise in resting membrane potential, occasionally followed by tonic spiking that fell silent once more (*N*=2) (Figure 9). As this did not happen with lower doses of ouabain used throughout this study (2 μM), we conclude that the dynamic Na^+/K^+ATPase that is activated by neuronal firing and interacts with Kv7 to regulate neuronal output through activity-dependent feedback. Altogether these results indicate that the dynamic Na^+/K^+ATPase and Kv7 channels are inversely co-expressed across a population of motoneurons to control firing rates through diverse feedback signals.

Figure 9: High Doses of Ouabain Target the Housekeeper Na^+/K^+ATPase

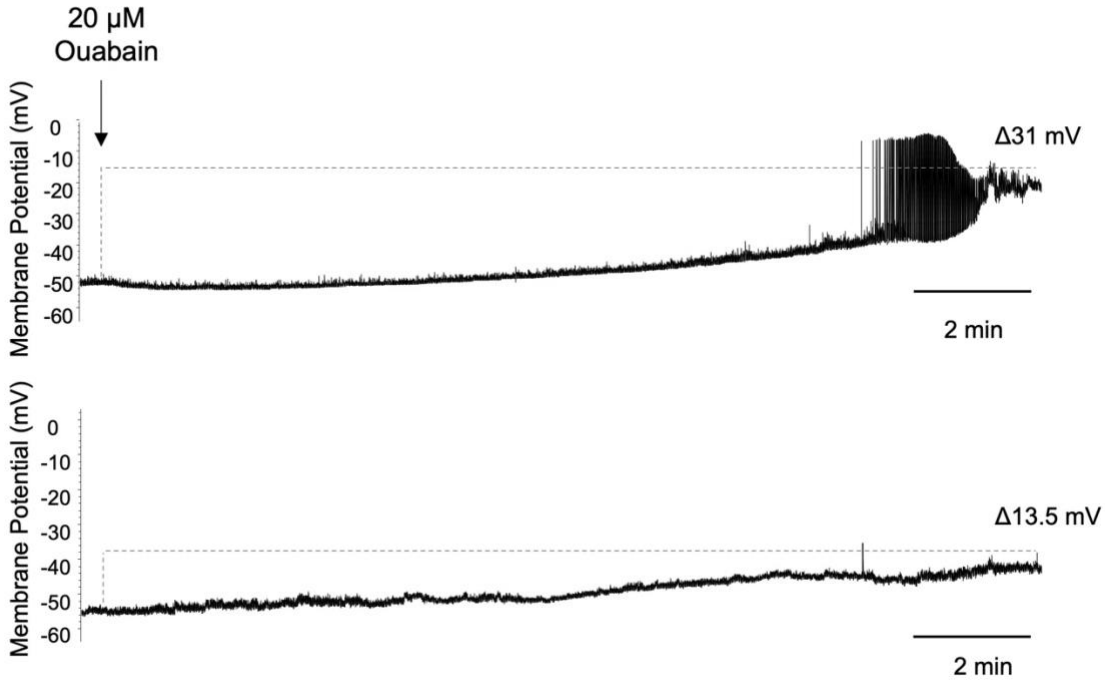

Treatment with 20 μM ouabain (10X the dosage used for all experiments in this study) caused dramatic depolarization and occasionally elicited tonic spiking (top trace). We concluded that 20 μM ouabain blocked the housekeeper Na^+/K^+ATPase and that our dose, 2 μM did not interfere with the activity of the housekeeper Na^+/K^+ATPase.

Discussion

The idea that neurons could adjust their ionic conductances in an activity-dependent manner as a response to an environmental perturbation appeared early in the 1990s where Franklin *et al* showed that Ca^{2+} currents were reduced during long treatment with high extracellular K^{+} (Franklin et al., 1992). Very soon, the idea that neurons could regulate all of their ionic conductances in an activity-dependent manner was put forth by Turrigiano and Marder after they observed neurons of the spiny lobster STG recovering their bursting ability following days in culture (G. Turrigiano et al., 1994; G. G. Turrigiano & Marder, 1993). One year later, this idea was supported by the same group (G. Turrigiano et al., 1994). Since then, both modeling and experimental work has shown that neurons regulate their ionic conductances in an activity-dependent fashion using just one activity sensor, intracellular calcium (Golowasch et al., 1999; Marder & Goaillard, 2006; Marder & Prinz, 2002; G. Turrigiano et al., 1995).

Research by O'Leary *et al* explored the possibility of two sensors for the regulation of neurons activity utilizing model cells and showed that the use of two sensors causes windup to occur because neither sensor was able to reach its target value simultaneously with the other (O'Leary et al., 2014). Windup is a phenomenon characterized by the uncontrolled regulation in a singular direction which causes overcompensation and loss of stability in the system (O'Leary et al., 2014). We can assume that windup would have disastrous consequences if it was occurring in a biological system (O'Leary et al., 2014). However, a number of regulatory mechanisms are present in different parts of the neuron, and it is entirely possible that the conservation of a broad trait, such as intrinsic excitability, arises from the combination of many small, "local" processes in different parts of the neuron (O'Leary & Wyllie, 2011).

Research in the STG and in model neurons has focused on regulation of intrinsic excitability over longer timescales (Golowasch et al., 1999; Marder & Goaillard, 2006; Marder & Prinz, 2002; G. Turrigiano et al., 1994). Research in Drosophila has utilized genetic perturbations to study intrinsic excitability over longer time scales (Apostolopoulou & Lin, 2020;

James et al., 2019). Regulation on shorter timescales, such as spike adaptation, also appear to rely on one sensor (Cao et al., 2015; Ha & Cheong, 2017). Spike adaptation in thalamocortical and hippocampal neurons relies on the influx of Ca^{2+} to activate calcium-activated chloride channels while spike adaptation in striatal output neurons appears to rely on voltage and is achieved via increased activity of the Kv7 channels (Cao et al., 2015; Ha et al., 2016; Ha & Cheong, 2017). Thus, most, if not all, literature to date operate under the implicit assumption that neurons of the same type use a dominant feedback system to regulate their activity over short and long timescales.

The experiments above contradict this precedent. We found that the dynamic Na^+/K^+ATPase and the Kv7 channel work together to produce the usAHP and regulate intrinsic excitability during physiological activity in the vagal motoneurons of the American Bullfrog. These findings are surprising for several reasons. First, our findings stand in direct opposition to previous theoretical and biological research which supports the hypothesis that neurons utilize one sensor to regulate their excitability on both shorter and longer timescales. Second, preliminary data confirms the potentiation of the Kv7 channel current while also showing that other K^+ currents are also potentiated by maximal stimuli. Third, we extend the concept of multiple solutions for cell-type specific output to activity-dependent feedback systems.

From our studies of the usAHP, we identified two sensors in our system: the dynamic Na^+/K^+ATPase and the Kv7 channel. The dynamic Na^+/K^+ATPase and the Kv7 channel appear to have their own target values for this timescale based upon their coexpression ratio. These two target values then combine to regulate activity. Why is it advantageous to have two sensors? Both of the ion transporters discussed here, the dynamic Na^+/K^+ATPase and Kv7 channels, rely on depletable substrates (ATP and PIP_2 respectively) therefore having a degenerate sensor may prove valuable in a situation where one substrate is depleted. Further, having varying proportions of these degenerate sensors in each neuron (different proportions in

each neuron) may function to keep the entire network stable in conditions that may deplete one of the necessary substrates.

What gaps currently exist in the model we put forward? Although the kinetics of Kv7 are slow relatively to other ion channels (100s of ms deactivation), a ~10-60s hyperpolarization caused by a channel seems too slow for a channel. However, our data show that XE-991 reduces the usAHP. How is this possible? Previous work has shown depolarization-dependent potentiation of Kv7 channels (Chen et al., 2011; X. Zhang et al., 2010). Zhang et al found that depolarization increased both PIP_2 levels and the Kv7 channel current through the increased activation of P14 kinase through genetic knockdown of P14 kinase (X. Zhang et al., 2010). Soon after, Chen *et al* found that depolarization increased the activity of protein kinase C (PKC), which in turn increased the synthesis of PIP_2 and caused an increase in the Kv7 channel current. The role of PKC was determined by both pharmacological and genetic means, with block of PKC by an inhibitor and RNA interference of P14 kinase, which interacts with PKC, attenuating the effect on PIP_2 levels and Kv7 channel current potentiation (Chen et al., 2011). Therefore, we conducted preliminary experiments where we measured the potentiation of the Kv7 current following brief depolarization. These preliminary results indicate that the Kv7 current is potentiated by sustained depolarization in voltage clamp mimicking the depolarization we used in current clamp to simulate maximal activity (Figure 10). The Kv7 current was substantially larger following the long depolarization in cells with a larger R_{in} Drop. The size of the37urrentt slowly decayed back to baseline over the minute-long recovery period. Although we identified as Kv7 component, other currents appear to be potentiated as well, suggesting further complexity in activity-dependent feedback regulation than just two sensory molecules (Figure 10).

Figure 10: Kv7 Channel Current Potentiation

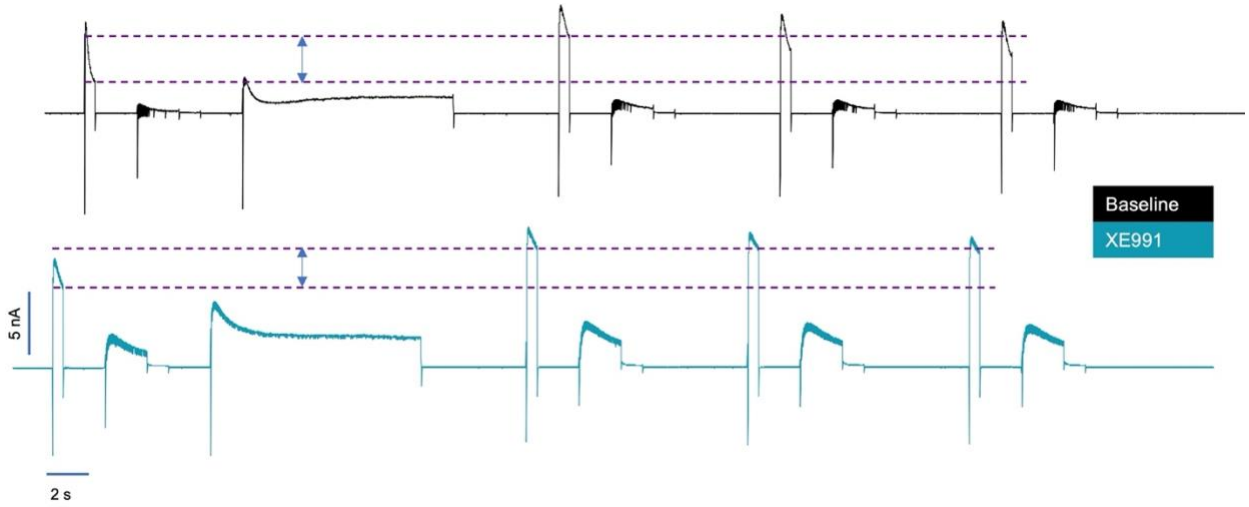

We evoked the outward K^+ current before and after a long depolarizing step that mimicked a maximal stimulus and found that the outward K^+ current was potentiated following the long depolarizing step (black trace, space between purple dotted lines). We found that this potentiation was reduced by the Kv7 channel blocker XE991 (blue trace). However, it was not completely gone and therefore we suspect that other outward K^+ currents are also potentiated by a maximal stimulus (space between purple lines, blue trace).

Finally, we documented a surprising amount of variation in the functional expression of the dynamic Na^+/K^+ATPase and Kv7 channels. These data indicate that each individual cell had a unique level of contribution from both the dynamic Na^+/K^+ATPase and the Kv7 channel in generating rapid feedback for firing rate control. Our results suggest that neurons can have varying combinations of ion transporters relates to ionic current correlations seen in other neurons systems. Prinz *et al* demonstrated that neurons in the STG that perform the exact same function can achieve their characteristic outputs with a staggering variety of combinations of the Na^+, K^+, and Ca^{2+} conductances (Prinz et al., 2004). In the STG, every neuron has been extensively characterized and is sometimes the only one of its kind in the animal (for example, there is only one AB neuron per animal), therefore studies in the STG have shown that the exact same neuron can achieve its characteristic output with different combinations of ion channels (Marder & Goaillard, 2006; Marder & Prinz, 2002). The variability in ionic conductances appears to be constrained by coexpression relationships, such as those already established for I_A and I_{KCa} as well as for I_A and I_H (MacLean et al., 2005; Ransdell et al., 2012). Our data support the restriction of variability through coexpression relationships, as the dynamic Na^+/K^+ATPase and Kv7 channels appear to be reciprocally co-expressed, generating a similar usAHP across neurons. Why so much variation exists has yet to be conclusively answered in the STG, but it has been surmised that variability endows the network with strength and flexibility and may give the organism more evolutionary potential and protection from mutations (Drion et al., 2015; Marder & Goaillard, 2006; Nelson & Turrigiano, 2008).

Conclusions and Implications

While vagal motoneurons all can regulate firing rates through negative feedback, they do not achieve this end via the same mechanisms. Instead of a single mechanism, or even a single combination, each neuron has its own unique solution for activity dependent-feedback using the dynamic Na^+ pump and Kv7. Given that these two mechanisms respond to different aspects of neuronal activity (intracellular Na^+ and membrane depolarization), our work has opens up the

possibility neurons in the same population simultaneously transduce their activity through multiple signals in differing proportions. Thus, our results demonstrate that feedback control may represent an emergent property, with coordinated expression of different feedback sensors in different amounts to define firing rate set-points of neurons.

The presence of two sensors and the variability both across the cell population within the same animal and between animals may mean that the presentation and treatment of neurological conditions such as Parkinson's and Alzheimer's Disease, and others is more complicated than is currently thought. For instance, while both the dynamic Na^+/K^+ATPase and the Kv7 channels have been implicated in Alzheimer's, treatments targeting only one of these ion transporters have resulted in varied responses (Nordberg, 1999; Shrivastava et al., 2020). Further, treatment with XE991 to prevent dopaminergic neuronal death in models of Parkinson's Disease has also had variable results (H. Liu et al., 2018). This may explain the variations in severity and progression of these diseases as well as offer insight as to why drugs that were made to combat these diseases did not live up to their predicted efficacies in human trials.

Our work introduces the idea that firing rate homeostasis can arise from combinations of feedback sensors. However, it leaves several important questions unanswered. How do longer-term mechanisms of intrinsic excitability regulation interact with or control the expression of shorter-term mechanisms described here? How does the variability in ionic conductances arise? What are the specific advantages of using combinations of two feedback sensors for the control of firing rate? Do two-sensor systems exist in other organisms? What developmental events determine if a neuron will have one or two sensors and how are they maintained? Each of these fundamental questions are central to understanding how neurons regulate their output in health and disease.

CHAPTER III: FUTURE DIRECTIONS

What are the practical implications of our results?

While the results of this study demonstrated the importance of both the dynamic Na^+/K^+ATPase and the Kv7 channels in the regulation of firing at the single neuron level, we have yet to determine how the disruption of these processes impacts the function of the circuit as a whole. The removal of either the dynamic Na^+/K^+ATPase, the Kv7 channels, or both increased average firing frequency but how this affects the overall output of the motor pool, i.e., recruitment of the population of motoneurons that activate the glottis during a breath, is still unknown. The lab does have a semi-intact preparation that would allow us to test this directly (Amaral-Silva & Santin, 2022). We could determine the circuit-level implications by recording motor output from the laryngeal branch of the CNX complex while patch clamping individual motoneurons and delivering the pharmacological agents used in this study (ouabain and XE991) directly to the vagal motor pool. In doing so, we might expect that the amplitude or frequency of the lung bursts increases and draw conclusions about how that impacts breathing in the whole animal.

More than just Kv7?

Our finding that activity potentiates the Kv7 channel current on such a fast time scale was surprising (Fig 10). However, during these experiments we also found that other outward K^+ currents were also potentiated by maximal stimuli, which was especially clear following treatment with XE991, where the outward K^+ current potentiation remained visibly obvious (Fig 10). Based on the kinetics of these currents, we predict they may involve Kv2 and Kv1 channels (Delgado-Ramírez et al., 2018, p. 2; Rezazadeh et al., 2007). To begin uncovering the channels behind this, we could employ specific blockers of these different channels. Kv2 channels also possess slow activation times and rely on membrane PIP_2 levels to avoid closed-state inactivation (Delgado-Ramírez et al., 2018). Kv2.2 channels have also been found in a related

frog genus, *Xenopus* (Burger & Ribera, 1996). Importantly, Kv2 channels have been implicated in the regulation of excitability, specifically by allowing neurons to maintain repetitive firing (Delgado-Ramírez et al., 2018; Romer et al., 2019). We could use the tarantula venom toxin, stromatoxin to determine if the cells possess a Kv2 channel current and if this current contributes to the outward K^+ current potentiation we have observed previously. This would be done using two separate protocols, a step protocol to maximally activate Kv2 channels and the same protocol used for the outward K^+ current potentiation. Kv1 channels can have slow activation/deactivation kinetics and are blocked by the sea anemone toxin, ShK (Zhao et al., 2015). These channels also play a key role in the regulation of intrinsic excitability (Rezazadeh et al., 2007).

How are short-term feedback mechanisms controlled by long-term perturbations such as overwintering?

In nature, bullfrogs are known to spend the winter months in ice-covered ponds. During the overwintering period, the frogs rely on cutaneous respiration to fulfill their gas exchange needs (Santin et al., 2017). The use of cutaneous respiration means that the circuit responsible for the generation of lung breathing is quiet for the duration of the overwintering (Santin et al., 2017). Generally speaking, when neural circuits are quiet or unused, they are harder to activate (Santin et al., 2017). But, contrary to this proven paradigm, the respiratory circuit of the bullfrog turns on with no issue following emergence from overwintering (Santin et al., 2017).

Previous studies from our lab have shown that long-term activity challenges during the winter leads to compensation that increases synaptic strength, which suggests increased excitability, in vagal motoneurons following overwintering (Santin et al., 2017; Zubov et al., 2022). How the neuron regulates this increase in excitability is still unknown to us. We have preliminary evidence that the usAHP is reduced following overwintering, which suggests that long-term compensation may alter the function of short-term feedback mechanisms to boost excitability. Experiments exactly like those already conducted to measure the usAHP in this

thesis could be used to determine the presence or absence of the usAHP in overwintered frogs. Regardless of the outcome of these experiments, the same experiments to determine the presence of the Kv7 channel current and the physiological protocol should be completed. We expect to see a change in the contribution of the dynamic Na^+/K^+ATPase to the regulation of intrinsic excitability based upon the preliminary observation that the usAHP is reduced. However, we are unsure of whether the Kv7 channel density increases to compensate for this change or if another ion transporter increases in density or function. It is also possible that the preliminary observations indicate the opposite situation, where the Kv7 channel density has fallen following overwintering. To determine this, the first step would be the analysis of membrane conductance before and after stimulation, as was done in the first results section.

The dynamic Na^+/K^+ATPase and Kv7 channels are co-expressed: Are they coregulated?

Finally, we would like to more about the coexpression relationship between the dynamic Na^+/K^+ATPase and Kv7 channels by investigating how they are coregulated. To do this, we could perform a similar experiment as that done by Ransdell et al (Ransdell et al., 2012). We could continuously treat the vagal motor pool with either ouabain or XE991 for a few hours and measure the usAHP, Kv7 channel densities, and rerun the physiological protocols at regular intervals during the treatment period. We expect to observe an initial increase in excitability due to the application of the pharmacological agents followed by a gradual return to normal activity levels. If activity is able to return to normal levels following long-term application of either ouabain or XE991, we can investigate the cellular signaling pathways that allowed this to occur, as well as if compensatory channels/pumps that were placed in the membrane to compensate for the loss of either the Kv7 channel or the dynamic Na^+/K^+ATPase.

Limitations and Alternative Follow-up Approaches

Confirming the absence of a role for Ca^{2+}in the usAHP

In Chapter II, we were able to rule out Ca^{2+} as a mechanism for the usAHP using 30 μM Cd^{2+}. This dose of Cd^{2+} is below the standard dose, which is approximately 100-300 μM (Huang

et al., 2012; Lett et al., 2017; Ransdell et al., 2012). We chose our dose based on the observation that higher doses of Cd^{2+} impacted cell excitability and were often difficult to get fully into our bicarbonate-buffered aCSF. Therefore, to ensure that our dose of Cd^{2+} was blocking voltage gated Ca^{2+} channels to a substantial degree, we will measure Ca^{2+} currents before and after application of 30 μM Cd^{2+}. Based on previous data, however, we expect this dose blocks 50-70% of the total Ca^{2+} current (*CaV2.2*, n.d.; Tsintsadze et al., 2017). Assuming we blocked a meaningful amount of the Ca^{2+} current using Cd^{2+}, our experiments still do not account for the possible of spikes in Ca^{2+} from intracellular stores. An alternative approach to address this issue would be to backfill patch pipettes with the Ca^{2+} chelator, BAPTA, to chelate intracellular Ca^{2+} during stimulation. This experiment also has its drawbacks, namely that dialysis of patch pipette contents into the cell is basically instantaneous, therefore each cell could not serve as its own control. We expect that our dose of Cd^{2+} was appropriate and that experiments with BAPTA will not be significantly different. We also expect that 30 μM Cd^{2+} will significantly block voltage gated Ca^{2+} channel currents.

Future Directions in the Hypoglossal Motor Pool

Why do these neurons not possess the usAHP?

Hypoglossal motoneurons do not appear to have the usAHP, but this finding is not uncommon in motoneurons. It has been shown that for some neurons, a current known as I_H, a hyperpolarization-activated mixed cation current that is produced by the activity of HCN channels, masks the usAHP in certain cells (Picton et al., 2018). This is because depolarizing HCN channels activate during membrane hyperpolarization and would serve to balance out the usAHP. Therefore, we could assess the presence/absence of I_H. If I_H is present, we could block I_H pharmacologically with ZD7288 or low mM cesium and attempt to evoke the usAHP to determine if I_H is indeed masking the usAHP in these cells. If these cells do not have I_H or if I_H is

present but not masking the usAHP, then we could potentially investigate the other AHPs as a measure of intrinsic excitability regulation.

How do other hypoglossal motoneurons dynamically regulate their intrinsic excitability?

Hypoglossal motoneurons play an important role in breathing and understanding how they regulate their intrinsic excitability could provide more support for our two-sensor model. To assess the generality of the usAHP in feedback control of firing rate across motor pools, we could collect this data using the semi-intact preparation using the same methods used for vagal motoneurons (Amaral-Silva & Santin, 2022). But we would not be able to repeat the experiments using the physiological protocol in Chapter II without understanding which ion transporters are necessary for a tractable measure of intrinsic excitability regulation, such as the usAHP or sAHP. Additionally, it is certainly possible that synaptic dynamics play a larger role in the intrinsic excitability regulation and that there is no masked usAHP. To determine if this is the case, we could analyze synaptic dynamics by investigating synaptic measures of excitability such as mini excitatory post-synaptic currents (mEPSCs) during physiologically relevant activity using the semi-intact preparation.

REFERENCES

Amaral-Silva, L., & Santin, J. M. (2022). A brainstem preparation allowing simultaneous access to respiratory motor output and cellular properties of motoneurons in American bullfrog. *The Journal of Experimental Biology*, jeb.244079. https://doi.org/10.1242/jeb.244079

Apostolopoulou, A. A., & Lin, A. C. (2020). Mechanisms underlying homeostatic plasticity in the Drosophila mushroom body in vivo. *Proceedings of the National Academy of Sciences of the United States of America*, *117*(28), 16606–16615. https://doi.org/10.1073/pnas.1921294117

Benned-Jensen, T., Christensen, R. K., Denti, F., Perrier, J.-F., Rasmussen, H. B., & Olesen, S.-P. (2016). Live Imaging of Kv7.2/7.3 Cell Surface Dynamics at the Axon Initial Segment: High Steady-State Stability and Calpain-Dependent Excitotoxic Downregulation Revealed. *The Journal of Neuroscience: The Official Journal of the Society for Neuroscience*, *36*(7), 2261–2266. https://doi.org/10.1523/JNEUROSCI.2631-15.2016

Bergquist, S., Dickman, D. K., & Davis, G. W. (2010). A hierarchy of cell intrinsic and target-derived homeostatic signaling. *Neuron*, *66*(2), 220–234. https://doi.org/10.1016/j.neuron.2010.03.023

Borde, M., Cazalets, J. R., & Buño, W. (1995). Activity-dependent response depression in rat hippocampal CA1 pyramidal neurons in vitro. *Journal of Neurophysiology*, *74*(4), 1714–1729. https://doi.org/10.1152/jn.1995.74.4.1714

Brown, D. A., & Adams, P. R. (1980). Muscarinic suppression of a novel voltage-sensitive K+ current in a vertebrate neurone. *Nature*, *283*(5748), 673–676. https://doi.org/10.1038/283673a0

Brown, D. A., & Passmore, G. M. (2009). Neural KCNQ (Kv7) channels. *British Journal of Pharmacology*, *156*(8), 1185–1195. https://doi.org/10.1111/j.1476-5381.2009.00111.x

Burger, C., & Ribera, A. B. (1996). Xenopus spinal neurons express Kv2 potassium channel transcripts during embryonic development. *The Journal of Neuroscience: The Official Journal of the Society for Neuroscience*, *16*(4), 1412–1421.

Cao, Y., Bartolomé-Martín, D., Rotem, N., Rozas, C., Dellal, S. S., Chacon, M. A., Kadriu, B., Gulinello, M., Khodakhah, K., & Faber, D. S. (2015). Rescue of homeostatic regulation of striatal excitability and locomotor activity in a mouse model of Huntington's disease. *Proceedings of the National Academy of Sciences*, *112*(7), 2239–2244. https://doi.org/10.1073/pnas.1405748112

CaV2.2. (n.d.). Retrieved June 28, 2022, from https://www.nanion.de/en/application-database/database-sorted-by-targets/cav2-2.html

Chen, X., Yuan, L.-L., Zhao, C., Birnbaum, S. G., Frick, A., Jung, W. E., Schwarz, T. L., Sweatt, J. D., & Johnston, D. (2006). Deletion of Kv4.2 gene eliminates dendritic A-type K+ current and enhances induction of long-term potentiation in hippocampal CA1 pyramidal neurons. *The Journal of Neuroscience: The Official Journal of the Society for Neuroscience*, *26*(47), 12143–12151. https://doi.org/10.1523/JNEUROSCI.2667-06.2006

Chen, X., Zhang, X., Jia, C., Xu, J., Gao, H., Zhang, G., Du, X., & Zhang, H. (2011). Membrane Depolarization Increases Membrane PtdIns(4,5)P2 Levels through Mechanisms Involving PKC βII and PI4 Kinase. *Journal of Biological Chemistry*, *286*(46), 39760–39767. https://doi.org/10.1074/jbc.M111.289090

Church, T. W., Brown, J. T., & Marrion, N. V. (2019). B3-Adrenergic receptor-dependent modulation of the medium afterhyperpolarization in rat hippocampal CA1 pyramidal neurons. *Journal of Neurophysiology*, *121*(3), 773–784. https://doi.org/10.1152/jn.00334.2018

Cooper, E. C. (2011). Made for "anchorin": Kv7.2/7.3 (KCNQ2/KCNQ3) channels and the modulation of neuronal excitability in vertebrate axons. *Seminars in Cell & Developmental Biology*, *22*(2), 185–192. https://doi.org/10.1016/j.semcdb.2010.10.001

Delgado-Ramírez, M., De Jesús-Pérez, J. J., Aréchiga-Figueroa, I. A., Arreola, J., Adney, S. K., Villalba-Galea, C. A., Logothetis, D. E., & Rodríguez-Menchaca, A. A. (2018). Regulation of Kv2.1 channel inactivation by phosphatidylinositol 4,5-bisphosphate. *Scientific Reports*, *8*(1), 1769. https://doi.org/10.1038/s41598-018-20280-w

Delmas, P., & Brown, D. A. (2005). Pathways modulating neural KCNQ/M (Kv7) potassium channels. *Nature Reviews. Neuroscience*, *6*(11), 850–862. https://doi.org/10.1038/nrn1785

Drion, G., O'Leary, T., & Marder, E. (2015). Ion channel degeneracy enables robust and tunable neuronal firing rates. *Proceedings of the National Academy of Sciences*, *112*(38), E5361–E5370. https://doi.org/10.1073/pnas.1516400112

Dunn, A. R., & Kaczorowski, C. C. (2019). Regulation of intrinsic excitability: Roles for learning and memory, aging and Alzheimer's disease, and genetic diversity. *Neurobiology of Learning and Memory*, *164*, 107069. https://doi.org/10.1016/j.nlm.2019.107069

Dwivedi, D., & Bhalla, U. S. (2021). Physiology and Therapeutic Potential of SK, H, and M Medium AfterHyperPolarization Ion Channels. *Frontiers in Molecular Neuroscience*, *14*, 658435. https://doi.org/10.3389/fnmol.2021.658435

Franklin, J. L., Fickbohm, D. J., & Willard, A. L. (1992). Long-term regulation of neuronal calcium currents by prolonged changes of membrane potential. *The Journal of Neuroscience: The Official Journal of the Society for Neuroscience*, *12*(5), 1726–1735.

George, M. S., Abbott, L. F., & Siegelbaum, S. A. (2009). HCN hyperpolarization-activated cation channels inhibit EPSPs by interactions with M-type K(+) channels. *Nature Neuroscience*, *12*(5), 577–584. https://doi.org/10.1038/nn.2307

Golowasch, J., Abbott, L. F., & Marder, E. (1999). Activity-dependent regulation of potassium currents in an identified neuron of the stomatogastric ganglion of the crab Cancer borealis. *The Journal of Neuroscience: The Official Journal of the Society for Neuroscience*, *19*(20), RC33.

Greene, D. L., & Hoshi, N. (2017). Modulation of Kv7 channels and excitability in the brain. *Cellular and Molecular Life Sciences: CMLS*, *74*(3), 495–508. https://doi.org/10.1007/s00018-016-2359-y

Greene, D. L., Kang, S., & Hoshi, N. (2017). XE991 and Linopirdine Are State-Dependent Inhibitors for Kv7/KCNQ Channels that Favor Activated Single Subunits. *The Journal of Pharmacology and Experimental Therapeutics*, *362*(1), 177–185. https://doi.org/10.1124/jpet.117.241679

Gu, N., Vervaeke, K., Hu, H., & Storm, J. F. (2005). Kv7/KCNQ/M and HCN/h, but not KCa2/SK channels, contribute to the somatic medium after-hyperpolarization and excitability control in CA1 hippocampal pyramidal cells. *The Journal of Physiology*, *566*(Pt 3), 689–715. https://doi.org/10.1113/jphysiol.2005.086835

Ha, G. E., & Cheong, E. (2017). Spike Frequency Adaptation in Neurons of the Central Nervous System. *Experimental Neurobiology*, *26*(4), 179–185. https://doi.org/10.5607/en.2017.26.4.179

Ha, G. E., Lee, J., Kwak, H., Song, K., Kwon, J., Jung, S.-Y., Hong, J., Chang, G.-E., Hwang, E. M., Shin, H.-S., Lee, C. J., & Cheong, E. (2016). The Ca2+-activated chloride channel anoctamin-2 mediates spike-frequency adaptation and regulates sensory transmission in thalamocortical neurons. *Nature Communications*, *7*, 13791. https://doi.org/10.1038/ncomms13791

Hachoumi, L., Rensner, R., Richmond, C., Picton, L., Zhang, H., & Sillar, K. T. (2022). Bimodal modulation of short-term motor memory via dynamic sodium pumps in a vertebrate spinal cord. *Current Biology: CB*, *32*(5), 1038-1048.e2. https://doi.org/10.1016/j.cub.2022.01.012

Hernandez, C. C., Zaika, O., Tolstykh, G. P., & Shapiro, M. S. (2008). Regulation of neural KCNQ channels: Signalling pathways, structural motifs and functional implications. *The Journal of Physiology*, *586*(7), 1811–1821. https://doi.org/10.1113/jphysiol.2007.148304

Huang, W. C., Xiao, S., Huang, F., Harfe, B. D., Jan, Y. N., & Jan, L. Y. (2012). Calcium-activated chloride channels (CaCCs) regulate action potential and synaptic response in hippocampal neurons. *Neuron*, *74*(1), 179–192. https://doi.org/10.1016/j.neuron.2012.01.033

James, T. D., Zwiefelhofer, D. J., & Frank, C. A. (2019). Maintenance of homeostatic plasticity at the Drosophila neuromuscular synapse requires continuous IP3-directed signaling. *ELife*, *8*, e39643. https://doi.org/10.7554/eLife.39643

Jiang, L., Kosenko, A., Yu, C., Huang, L., Li, X., & Hoshi, N. (2015). Activation of m1 muscarinic acetylcholine receptor induces surface transport of KCNQ channels through a CRMP-2-mediated pathway. *Journal of Cell Science*, *128*(22), 4235–4245. https://doi.org/10.1242/jcs.175547

Joseph, A., & Turrigiano, G. G. (2017). All for One But Not One for All: Excitatory Synaptic Scaling and Intrinsic Excitability Are Coregulated by CaMKIV, Whereas Inhibitory Synaptic Scaling Is Under Independent Control. *The Journal of Neuroscience: The Official Journal of the Society for Neuroscience*, *37*(28), 6778–6785. https://doi.org/10.1523/JNEUROSCI.0618-17.2017

Kaczmarek, L. K. (1987). The role of protein kinase C in the regulation of ion channels and neurotransmitter release. *Trends in Neurosciences*, *10*(1), 30–34. https://doi.org/10.1016/0166-2236(87)90122-6

Kogo, N., Perry, S. F., & Remmers, J. E. (1994). Neural organization of the ventilatory activity in the frog, Rana catesbeiana. I. *Journal of Neurobiology*, *25*(9), 1067–1079. https://doi.org/10.1002/neu.480250904

Kogo, N., & Remmers, J. E. (1994). Neural organization of the ventilatory activity in the frog, Rana catesbeiana. II. *Journal of Neurobiology*, *25*(9), 1080–1094. https://doi.org/10.1002/neu.480250905

LeMasson, G., Marder, E., & Abbott, L. F. (1993). Activity-dependent regulation of conductances in model neurons. *Science (New York, N.Y.)*, *259*(5103), 1915–1917. https://doi.org/10.1126/science.8456317

Lett, K. M., Garcia, V. J., Temporal, S., Bucher, D., & Schulz, D. J. (2017). Removal of endogenous neuromodulators in a small motor network enhances responsiveness to neuromodulation. *Journal of Neurophysiology*, *118*(3), 1749–1761. https://doi.org/10.1152/jn.00383.2017

Lignani, G., Baldelli, P., & Marra, V. (2020). Homeostatic Plasticity in Epilepsy. *Frontiers in Cellular Neuroscience*, *14*, 197. https://doi.org/10.3389/fncel.2020.00197

Liu, H., Jia, L., Chen, X., Shi, L., & Xie, J. (2018). The Kv7/KCNQ channel blocker XE991 protects nigral dopaminergic neurons in the 6-hydroxydopamine rat model of Parkinson's disease. *Brain Research Bulletin*, *137*, 132–139. https://doi.org/10.1016/j.brainresbull.2017.11.011

Liu, Z., Golowasch, J., Marder, E., & Abbott, L. F. (1998). A model neuron with activity-dependent conductances regulated by multiple calcium sensors. *The Journal of Neuroscience: The Official Journal of the Society for Neuroscience*, *18*(7), 2309–2320.

MacLean, J. N., Zhang, Y., Goeritz, M. L., Casey, R., Oliva, R., Guckenheimer, J., & Harris-Warrick, R. M. (2005). Activity-independent coregulation of IA and Ih in rhythmically active neurons. *Journal of Neurophysiology*, *94*(5), 3601–3617. https://doi.org/10.1152/jn.00281.2005

Marder, E., & Goaillard, J.-M. (2006). Variability, compensation and homeostasis in neuron and network function. *Nature Reviews. Neuroscience*, *7*(7), 563–574. https://doi.org/10.1038/nrn1949

Marder, E., & Prinz, A. A. (2002). Modeling stability in neuron and network function: The role of activity in homeostasis. *BioEssays: News and Reviews in Molecular, Cellular and Developmental Biology*, *24*(12), 1145–1154. https://doi.org/10.1002/bies.10185

Nelson, S. B., & Turrigiano, G. G. (2008). Strength through diversity. *Neuron*, *60*(3), 477–482. https://doi.org/10.1016/j.neuron.2008.10.020

Niday, Z., & Bean, B. P. (2021). BK Channel Regulation of Afterpotentials and Burst Firing in Cerebellar Purkinje Neurons. *The Journal of Neuroscience: The Official Journal of the Society for Neuroscience*, *41*(13), 2854–2869. https://doi.org/10.1523/JNEUROSCI.0192-20.2021

Nordberg, A. (1999). PET studies and cholinergic therapy in Alzheimer's disease. *Revue Neurologique*, *155 Suppl 4*, S53-63.

O'Leary, T., Williams, A. H., Franci, A., & Marder, E. (2014). Cell types, network homeostasis, and pathological compensation from a biologically plausible ion channel expression model. *Neuron*, *82*(4), 809–821. https://doi.org/10.1016/j.neuron.2014.04.002

O'Leary, T., & Wyllie, D. J. A. (2011). Neuronal homeostasis: Time for a change? *The Journal of Physiology*, *589*(Pt 20), 4811–4826. https://doi.org/10.1113/jphysiol.2011.210179

Picton, L. D., Nascimento, F., Broadhead, M. J., Sillar, K. T., & Miles, G. B. (2017). Sodium Pumps Mediate Activity-Dependent Changes in Mammalian Motor Networks. *The Journal of Neuroscience*, *37*(4), 906–921. https://doi.org/10.1523/JNEUROSCI.2005-16.2016

Picton, L. D., Sillar, K. T., & Zhang, H.-Y. (2018). Control of Xenopus Tadpole Locomotion via Selective Expression of Ih in Excitatory Interneurons. *Current Biology: CB*, *28*(24), 3911-3923.e2. https://doi.org/10.1016/j.cub.2018.10.048

Picton, L. D., Zhang, H., & Sillar, K. T. (2017). Sodium pump regulation of locomotor control circuits. *Journal of Neurophysiology*, *118*(2), 1070–1081. https://doi.org/10.1152/jn.00066.2017

Prinz, A. A., Bucher, D., & Marder, E. (2004). Similar network activity from disparate circuit parameters. *Nature Neuroscience*, *7*(12), 1345–1352. https://doi.org/10.1038/nn1352

Pulver, S. R., & Griffith, L. C. (2010). Spike integration and cellular memory in a rhythmic network from Na+/K+ pump current dynamics. *Nature Neuroscience*, *13*(1), 53–59. https://doi.org/10.1038/nn.2444

Ransdell, J. L., Nair, S. S., & Schulz, D. J. (2012). Rapid Homeostatic Plasticity of Intrinsic Excitability in a Central Pattern Generator Network Stabilizes Functional Neural Network Output. *Journal of Neuroscience*, *32*(28), 9649–9658. https://doi.org/10.1523/JNEUROSCI.1945-12.2012

Rasmussen, H., & Barrett, P. Q. (1984). Calcium messenger system: An integrated view. *Physiological Reviews*, *64*(3), 938–984. https://doi.org/10.1152/physrev.1984.64.3.938

Rezazadeh, S., Kurata, H. T., Claydon, T. W., Kehl, S. J., & Fedida, D. (2007). An activation gating switch in Kv1.2 is localized to a threonine residue in the S2-S3 linker. *Biophysical Journal*, *93*(12), 4173–4186. https://doi.org/10.1529/biophysj.107.116160

Rodríguez-Menchaca, A. A., Adney, S. K., Zhou, L., & Logothetis, D. E. (2012). Dual Regulation of Voltage-Sensitive Ion Channels by PIP(2). *Frontiers in Pharmacology*, *3*, 170. https://doi.org/10.3389/fphar.2012.00170

Romer, S. H., Deardorff, A. S., & Fyffe, R. E. W. (2019). A molecular rheostat: Kv2.1 currents maintain or suppress repetitive firing in motoneurons. *The Journal of Physiology*, *597*(14), 3769–3786. https://doi.org/10.1113/JP277833

Santin, J. M., Vallejo, M., & Hartzler, L. K. (2017). Synaptic up-scaling preserves motor circuit output after chronic, natural inactivity. *ELife*, *6*, e30005. https://doi.org/10.7554/eLife.30005

Sheng, M., & Greenberg, M. E. (1990). The regulation and function of c-fos and other immediate early genes in the nervous system. *Neuron*, *4*(4), 477–485. https://doi.org/10.1016/0896-6273(90)90106-p

Shmukler, B. E., Bond, C. T., Wilhelm, S., Bruening-Wright, A., Maylie, J., Adelman, J. P., & Alper, S. L. (2001). Structure and complex transcription pattern of the mouse SK1 K(Ca)

channel gene, KCNN1. *Biochimica Et Biophysica Acta*, *1518*(1–2), 36–46. https://doi.org/10.1016/s0167-4781(01)00166-x

Shrivastava, A. N., Triller, A., & Melki, R. (2020). Cell biology and dynamics of Neuronal Na+/K+-ATPase in health and diseases. *Neuropharmacology*, *169*, 107461. https://doi.org/10.1016/j.neuropharm.2018.12.008

Storm, J. F. (1989). An after-hyperpolarization of medium duration in rat hippocampal pyramidal cells. *The Journal of Physiology*, *409*, 171–190. https://doi.org/10.1113/jphysiol.1989.sp017491

Tiwari, M. N., Mohan, S., Biala, Y., & Yaari, Y. (2019). Protein Kinase A-Mediated Suppression of the Slow Afterhyperpolarizing KCa3.1 Current in Temporal Lobe Epilepsy. *The Journal of Neuroscience: The Official Journal of the Society for Neuroscience*, *39*(50), 9914–9926. https://doi.org/10.1523/JNEUROSCI.1603-19.2019

Trasande, C. A., & Ramirez, J.-M. (2007). Activity deprivation leads to seizures in hippocampal slice cultures: Is epilepsy the consequence of homeostatic plasticity? *Journal of Clinical Neurophysiology: Official Publication of the American Electroencephalographic Society*, *24*(2), 154–164. https://doi.org/10.1097/WNP.0b013e318033787f

Tsintsadze, T., Williams, C. L., Weingarten, D. J., Gersdorff, H. von, & Smith, S. M. (2017). Distinct Actions of Voltage-Activated Ca2+ Channel Block on Spontaneous Release at Excitatory and Inhibitory Central Synapses. *Journal of Neuroscience*, *37*(16), 4301–4310. https://doi.org/10.1523/JNEUROSCI.3488-16.2017

Turrigiano, G., Abbott, L. F., & Marder, E. (1994). Activity-dependent changes in the intrinsic properties of cultured neurons. *Science (New York, N.Y.)*, *264*(5161), 974–977. https://doi.org/10.1126/science.8178157

Turrigiano, G. G., & Marder, E. (1993). Modulation of identified stomatogastric ganglion neurons in primary cell culture. *Journal of Neurophysiology*, *69*(6), 1993–2002. https://doi.org/10.1152/jn.1993.69.6.1993

Turrigiano, G., LeMasson, G., & Marder, E. (1995). Selective regulation of current densities underlies spontaneous changes in the activity of cultured neurons. *The Journal of Neuroscience: The Official Journal of the Society for Neuroscience*, *15*(5 Pt 1), 3640–3652.

Vallejo, M., Santin, J. M., & Hartzler, L. K. (2018). Noradrenergic modulation determines respiratory network activity during temperature changes in the in vitro brainstem of bullfrogs. *Respiratory Physiology & Neurobiology*, *258*, 25–31. https://doi.org/10.1016/j.resp.2018.10.002

Vatanparast, J., & Janahmadi, M. (2009). Contribution of apamin-sensitive SK channels to the firing precision but not to the slow afterhyperpolarization and spike frequency adaptation in snail neurons. *Brain Research*, *1255*, 57–66. https://doi.org/10.1016/j.brainres.2008.12.003

Vervaeke, K., Gu, N., Agdestein, C., Hu, H., & Storm, J. F. (2006). Kv7/KCNQ/M-channels in rat glutamatergic hippocampal axons and their role in regulation of excitability and transmitter release. *The Journal of Physiology*, *576*(Pt 1), 235–256. https://doi.org/10.1113/jphysiol.2006.111336

Wiener, N. (2019). *Cybernetics or Control and Communication in the Animal and the Machine, Reissue of the 1961 second edition*. MIT Press.

Zenke, F., & Gerstner, W. (2017). Hebbian plasticity requires compensatory processes on multiple timescales. *Philosophical Transactions of the Royal Society of London. Series B, Biological Sciences*, *372*(1715), 20160259. https://doi.org/10.1098/rstb.2016.0259

Zhang, H.-Y., Picton, L., Li, W.-C., & Sillar, K. T. (2015). Mechanisms underlying the activity-dependent regulation of locomotor network performance by the Na+ pump. *Scientific Reports*, *5*, 16188. https://doi.org/10.1038/srep16188

Zhang, H.-Y., & Sillar, K. T. (2012). Short-term memory of motor network performance via activity-dependent potentiation of Na+/K+ pump function. *Current Biology: CB*, *22*(6), 526–531. https://doi.org/10.1016/j.cub.2012.01.058

Zhang, J., Chen, X., Xue, Y., Gamper, N., & Zhang, X. (2018). Beyond voltage-gated ion channels: Voltage-operated membrane proteins and cellular processes. *Journal of Cellular Physiology*, *233*(10), 6377–6385. https://doi.org/10.1002/jcp.26555

Zhang, X., Chen, X., Jia, C., Geng, X., Du, X., & Zhang, H. (2010). Depolarization Increases Phosphatidylinositol (PI) 4,5-Bisphosphate Level and KCNQ Currents through PI 4-Kinase Mechanisms *. *Journal of Biological Chemistry*, *285*(13), 9402–9409. https://doi.org/10.1074/jbc.M109.068205

Zhao, Y., Huang, J., Yuan, X., Peng, B., Liu, W., Han, S., & He, X. (2015). Toxins Targeting the Kv1.3 Channel: Potential Immunomodulators for Autoimmune Diseases. *Toxins*, *7*(5), 1749–1764. https://doi.org/10.3390/toxins7051749

Zubov, T., Amaral-Silva, L. do, & Santin, J. M. (2022). *Inactivity and Ca2+ signaling regulate synaptic compensation in motoneurons following hibernation in American bullfrogs* (p. 2022.01.26.477843). bioRxiv. https://doi.org/10.1101/2022.01.26.477843

Zubov, T., Silika, S., Dukkipati, S. S., Hartzler, L. K., & Santin, J. M. (2021). Characterization of laryngeal motor neuron properties in the American bullfrog, Lithobates catesbieanus. *Respiratory Physiology & Neurobiology*, *294*, 103745. https://doi.org/10.1016/j.resp.2021.103745